MAVIS: Mathematical Visual Instruction Tuning with an Automatic Data Engine

Renrui Zhang[1*†], **Xinyu Wei**[3*], **Dongzhi Jiang**[1], **Ziyu Guo**[2], **Yichi Zhang**[3], **Chengzhuo Tong**[4]
Jiaming Liu[3], **Aojun Zhou**[1], **Shanghang Zhang**[3], **Peng Gao**[4], **Hongsheng Li**[1,5‡]

[1]CUHK MMLab & [2]MiuLar Lab [3]Peking University
[4]Shanghai AI Laboratory [5]CPII under InnoHK
renruizhang@link.cuhk.edu.hk, allen_wei@stu.pku.edu.cn

* Equal contribution † Project lead ‡ Corresponding author

Abstract

Multi-modal Large Language Models (MLLMs) have recently showcased superior proficiency in general visual scenarios. However, we identify their mathematical capabilities remain under-explored with three areas to be improved: *visual encoding of math diagrams*, *diagram-language alignment*, and *chain-of-thought (CoT) reasoning*. This draws forth an urgent demand for an effective training paradigm and a large-scale, comprehensive dataset with detailed CoT rationales, which is challenging to collect and costly to annotate manually. To tackle this issue, we propose **MAVIS**, a **MA**thematical **VIS**ual instruction tuning pipeline for MLLMs, featuring an automatic data engine to efficiently create mathematical visual datasets. We design the data generation process to be entirely independent of human intervention or GPT API usage, while ensuring the diagram-caption correspondence, question-answer correctness, and CoT reasoning quality. With this approach, we curate two datasets, MAVIS-Caption (558K diagram-caption pairs) and MAVIS-Instruct (834K visual math problems with CoT rationales), and propose four progressive stages for training MLLMs from scratch. First, we utilize MAVIS-Caption to fine-tune a math-specific vision encoder (CLIP-Math) through contrastive learning, tailored for improved diagram visual encoding. Second, we also leverage MAVIS-Caption to align the CLIP-Math with a large language model (LLM) by a projection layer, enhancing vision-language alignment in mathematical domains. Third, we adopt MAVIS-Instruct to perform the instruction tuning for robust problem-solving skills, and term the resulting model as MAVIS-7B. Fourth, we apply Direct Preference Optimization (DPO) to enhance the CoT capabilities of our model, further refining its step-wise reasoning performance. On various mathematical benchmarks, our MAVIS-7B achieves leading results among open-source MLLMs, e.g., surpassing other 7B models by +9.3% and the second-best LLaVA-NeXT (110B) by +6.9%, demonstrating the effectiveness of our method. Data and models are released at https://github.com/ZrrSkywalker/MAVIS.

1 Introduction

The pursuit of artificial general intelligence necessitates models to seamlessly interpret and generate multi-modal data. In recent years, the advent of Large-language Models (LLMs) (Brown et al., 2020; Touvron et al., 2023a;b; Chiang et al., 2023) and their Multi-modal extension (MLLMs) (Zhang et al., 2024a; Gao et al., 2023b; Su et al., 2023; Ye et al., 2023a) have significantly facilitated this process across various fields, such as healthcare (Singhal et al., 2023; Shu et al., 2023), autonomous driving (Yang et al., 2023; Jin et al., 2024), and robotics (Li et al., 2023b; Liu et al., 2024b). Although MLLMs exhibit remarkable performance in diverse tasks and benchmarks, one arena where they have yet to fully demonstrate their potential is mathematical problem-solving in visual contexts.

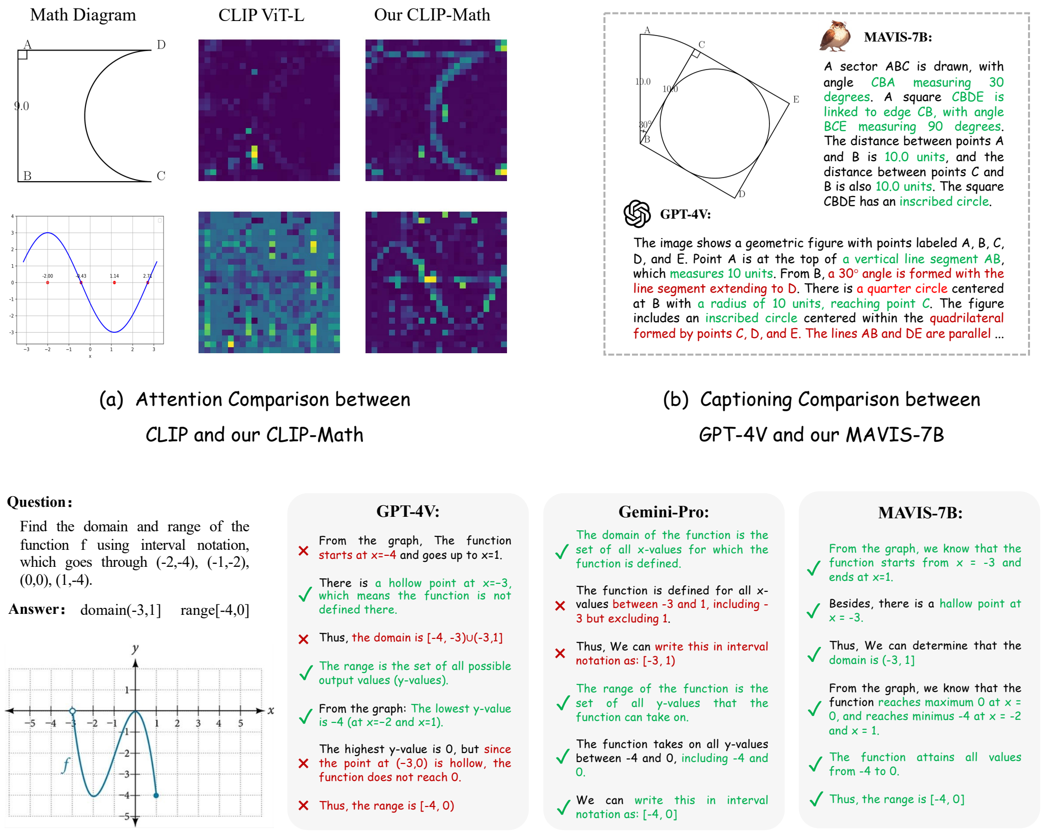

(a) Attention Comparison between CLIP and our CLIP-Math

MAVIS-7B:

A sector ABC is drawn, with angle CBA measuring 30 degrees. A square CBDE is linked to edge CB, with angle BCE measuring 90 degrees. The distance between points A and B is 10.0 units, and the distance between points C and B is also 10.0 units. The square CBDE has an inscribed circle.

GPT-4V:

The image shows a geometric figure with points labeled A, B, C, D, and E. Point A is at the top of a vertical line segment AB, which measures 10 units. From B, a 30° angle is formed with the line segment extending to D. There is a quarter circle centered at B with a radius of 10 units, reaching point C. The figure includes an inscribed circle centered within the quadrilateral formed by points C, D, and E. The lines AB and DE are parallel ...

(b) Captioning Comparison between GPT-4V and our MAVIS-7B

Question:

Find the domain and range of the function f using interval notation, which goes through (-2,-4), (-1,-2), (0,0), (1,-4).

Answer: domain(-3,1] range[-4,0]

GPT-4V:

✗ From the graph, The function starts at x=−4 and goes up to x=1.

✓ There is a hollow point at x=−3, which means the function is not defined there.

✗ Thus, the domain is [-4, -3)∪(-3,1]

✓ The range is the set of all possible output values (y-values).

✓ From the graph: The lowest y-value is −4 (at x=−2 and x=1).

✗ The highest y-value is 0, but since the point at (−3,0) is hollow, the function does not reach 0.

✗ Thus, the range is [-4, 0)

Gemini-Pro:

✓ The domain of the function is the set of all x-values for which the function is defined.

✗ The function is defined for all x-values between -3 and 1, including -3 but excluding 1.

✗ Thus, We can write this in interval notation as: [-3, 1)

✓ The range of the function is the set of all y-values that the function can take on.

✓ The function takes on all y-values between -4 and 0, including -4 and 0.

✓ We can write this in interval notation as: [-4, 0]

MAVIS-7B:

✓ From the graph, we know that the function starts from x = -3 and ends at x=1.

✓ Besides, there is a hallow point at x = -3.

✓ Thus, We can determine that the domain is (-3, 1]

✓ From the graph, we know that the function reaches maximum 0 at x = 0, and reaches minimus -4 at x = -2 and x = 1.

✓ The function attains all values from -4 to 0.

✓ Thus, the range is [-4, 0]

(c) CoT Reasoning Comparison between Different MLLMs

Figure 1: **(a)** We compare the attention map of class tokens from CLIP ViT-L (Radford et al., 2021) and our CLIP-Math. Our vision encoder can better capture significant mathematical information within diagrams. **(b)** We compare the diagram captioning capabilities between GPT-4V (OpenAI, 2023c) and our MAVIS-7B, where GPT-4V fall short of accurately recognizing mathematical elements. **(c)** We compare the chain-of-thought (CoT) reasoning between different models, showcasing that GPT-4V and Gemini-Pro (Gemini Team, 2023) suffer from low-quality reasoning process.

Existing efforts (OpenAI, 2023b;a; Zhou et al., 2023) for text-only mathematics have attained considerable progress, largely attributed to the availability of sufficient and easily accessible training data. In contrast, solving visual mathematical problems remains a significant challenge for MLLMs, primarily due to the absence of a fully validated, effective training pipeline and the acute shortage of large-scale, high-quality datasets. Visual mathematical data is not only more costly to collect from publicly available sources compared to text-only data, but also requires expensive manual annotation to produce accurate step-by-step chain-of-thought (CoT) rationales integrating diagram information. In light of these challenges, we identify three critical issues that impede the visual mathematical capabilities of MLLMs.

i. **Unsatisfactory math diagram embeddings by vision encoders.** Most MLLMs adopt a frozen CLIP (Radford et al., 2021) as the vision encoder, which is pre-trained by natural images capturing real-world scenes with rich colors and textures. In contrast, math diagrams are composed of abstract curves, shapes, and symbols with a monochromatic color scheme, exhibiting large semantic gaps to general scenarios. As visualized in Figure 1 (a), the attention map of CLIP struggles to capture important information within math diagrams, which cannot provide satisfactory visual embeddings for LLMs to understand.

ii. **Diagram-language misalignment between vision encoders and LLMs.** Likewise, the vision-language pre-training stage of MLLMs also adopts natural image-caption pairs for cross-modal alignment. Due to the domain gap, while they can generate accurate captions for real-world images, but fall short of recognizing basic mathematical elements and narrating their relations. As compared in Figure 1 (b), even GPT-4V (OpenAI, 2023c) produces low-quality descriptions for simple geometric figures and functions, indicating LLMs are not well aligned with the visual embedding space of math diagrams.

iii. **Inaccurate CoT reasoning capabilities with visual elements by MLLMs.** Referring to the CoT evaluation in MathVerse (Zhang et al., 2024b), incorporating the diagram input would adversely affect the reasoning quality of MLLMs compared to using only the text-only question. As visualized in Figure 1 (c), we observe the problem-solving process of GPT-4V and Gemini-Pro (Gemini Team, 2023) both suffer from low-quality CoT reasoning accuracy. This demonstrates the incapability of MLLMs to leverage visual cues for precise step-by-step mathematical problem-solving.

Therefore, to mitigate these issues, it is essential to develop an extensive dataset and effective training approach tailored to visual mathematics. In this paper, we propose **MAVIS**, a **MA**thematical **VIS**ual instruction tuning paradigm and an automatic data generation engine for MLLMs, which aims to fully unleash their potential for diagram visual encoding and reasoning capabilities. We introduce two meticulously curated datasets, a progressive four-stage training pipeline, and a visual mathematical specialist, MAVIS-7B. We summarize the contributions of our work as follows.

- **Automatic Mathematical Visual Data Engine.** To eliminate the need for labor-intensive annotation and expensive GPT API (OpenAI, 2023c;b) usage, we designed our data engine to be entirely rule-based and fully automated. This engine handles every aspect of mathematical data creation, including diagram drawing, caption generation, question-answer synthesis, and CoT rationale production. With this approach, we curate two large-scale, high-quality mathematical visual datasets, MAVIS-Caption and MAVIS-Instruct, widely covering plane geometry, analytic geometry, and function. MAVIS-Caption consists of 558K diagram-caption pairs automatically created by our data engine with accurate vision-language correspondence. MAVIS-Instruct includes 834K visual math problems, which includes 582K data constructed by our data engine and additional 252K data augmented by GPT-4V from manual collection and existing datasets (Chen et al., 2021c; Lu et al., 2021). Each problem is annotated with a CoT rationale, and modified to contain minimized textual redundancy that enforces MLLMs to pay more attention on visual diagrams.

- **Four-stage Training Pipeline.** Our training framework involves four progressive stages designed to sequentially address the aforementioned identified deficiencies in MLLMs. Firstly, we utilize MAVIS-Caption to fine-tune a math-specific vision encoder by contrastive learning, termed CLIP-Math, to enable better visual representations of math diagrams. Subsequently, we align this encoder with the LLM to ensure effective diagram-language integration also by MAVIS-Caption. After that, our MAVIS-Instruct is adopted to instruction-tune the MLLM, which provides sufficient step-wise problem-solving supervision. Finally, we employ Direct Preference Optimization (DPO) (Rafailov et al., 2024) with annotated CoT rationales in MAVIS-Instruct to further enhance the reasoning capabilities of our model.

- **Mathematical Visual Specialist.** After the four-stage training, we develop MAVIS-7B, an MLLM specifically optimized for visual mathematical problem-solving. On various evaluation benchmarks, our model achieves leading performance compared to existing open-source MLLMs, e.g., surpassing other 7B models by +9.3% and the second-best LLaVA-NeXT (110B) (Li et al., 2024a) by +6.9% on MathVerse (Zhang et al., 2024b). The quantitative results and qualitative analysis both validate the significance of our approach.

2 Automatic Data Engine

To cope with the substantial data requirements of MLLMs, it is essential to have access to extensive training instances. However, for visual mathematics, the paucity of publicly available datasets poses a challenge, and creating such data manually also involves a high cost. Therefore, as illustrated in Figure 2, we develop an automatic data engine to efficiently generate high-quality math diagrams (Section 2.1), captions (Section 2.2), and question-answer with rationales (Section 2.3).

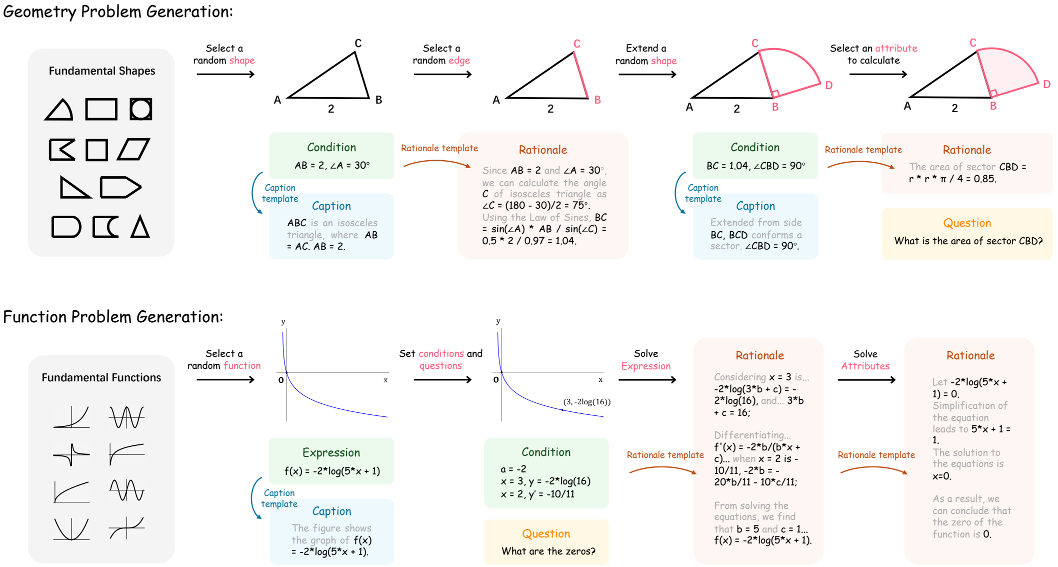
Geometry Problem Generation:
Fundamental Shapes
Select a random shape
C
A
2
B
Select a random edge
Extend a random shape
D
Select an attribute to calculate
Condition
AB = 2, ∠A = 30°
Caption template
Caption
ABC is an isosceles triangle, where AB = AC. AB = 2.
Rationale template
Rationale
Since AB = 2 and ∠A = 30°, we can calculate the angle C of isosceles triangle as ∠C = (180 - 30)/2 = 75°. Using the Law of Sines, BC = sin(∠A) * AB / sin(∠C) = 0.5 * 2 / 0.97 = 1.04.
Condition
BC = 1.04, ∠CBD = 90°
Caption template
Caption
Extended from side BC, BCD conforms a sector. ∠CBD = 90°.
Rationale template
Rationale
The area of sector CBD = r * r * π / 4 = 0.85.
Question
What is the area of sector CBD?
Function Problem Generation:
Fundamental Functions
Select a random function
y
0
x
Set conditions and questions
(3, -2log(16))
Expression
f(x) = -2*log(5*x + 1)
Caption template
Caption
The figure shows the graph of f(x) = -2*log(5*x + 1).
Condition
a = -2
x = 3, y = -2*log(16)
x = 2, y' = -10/11
Question
What are the zeros?
Solve Expression
Rationale template
Rationale
Considering x = 3 is... -2*log(3*b + c) = -2*log(16), and... 3*b + c = 16;
Differentiating... f'(x) = -2*b/(b*x + c)... when x = 2 is -10/11, -2*b = -20*b/11 - 10*c/11;
From solving the equations, we find that b = 5 and c = 1... f(x) = -2*log(5*x + 1).
Solve Attributes
Rationale template
Rationale
Let -2*log(5*x + 1) = 0. Simplification of the equation leads to 5*x + 1 = 1. The solution to the equations is x=0.
As a result, we can conclude that the zero of the function is 0.

Figure 2: **Overview of Automatic Data Engine.** We present the generation pipelines of geometry (Top) and function (Bottom) problems within the proposed automatic data engine, including diagrams, questions, captions, and Chain-of-Thought (CoT) rationales.

2.1 Diagram Generation

Covering most mathematical scenarios, we adopt three diagram types: plane geometry, analytic geometry, and function. Note that all the logic of the data engine is implemented in Python, and we employ Matplotlib for the graphical rendering of the diagrams.

Plane Geometry Diagram. As such diagrams typically consist of spatial combinations of various basic shapes, we utilize principles from multi-hop data curation to develop customized generation rules. These rules allow for the iterative integration of new shapes into existing configurations. Initially, we establish a core set of shapes, including squares, rectangles, triangles, sectors, etc, for diagram generation. Starting with a randomly selected shape, we extend another shape from the set along one of its straight sides. By iterating this process, we can construct diverse plane geometry diagrams featuring different combinations of shapes. Additionally, we randomly label the vertices with letters (e.g., A, B, C) and annotate numerical values relevant to geometric properties (e.g., side lengths and angles), simulating realistic plane geometry problems.

Analytic Geometry Diagram. Likewise, our approach begins by defining a basic figure set that differs slightly from that used in plane geometry; for example, we include additional elements such as points and line segments. We then construct a Cartesian coordinate system, complete with grid lines and scaled axes. The range of the coordinate system is randomly determined within a predefined scope. Subsequently, we select a number from 1 to 3 to indicate the number of figures to be drawn on the graph, and randomly choose coordinates for the top-left vertices to plot these figures at varied sizes (using these points as centers for circles). Unlike plane geometry, we ensure that the figures do not overlap, except for points and segments, and maintain the figure areas within a suitable scale.

Function Diagram. We focus on seven fundamental function types: polynomial, sine, cosine, tangent, logarithmic, absolute value, and piece-wise polynomial functions. For each function type, we parameterize the equations with random variables, such as coefficients and constants within a predefined range (e.g., a and b in $y = ax + b$), which facilitates the generation of diverse function graphs. We also adopt the same Cartesian coordinate system employed for analytic geometry. Additionally, for specific caption or question-answering samples, we also plot key features like extreme points and zero points of the functions, providing additional visual information that aids in the understanding and reasoning of these mathematical functions.

Diagram:

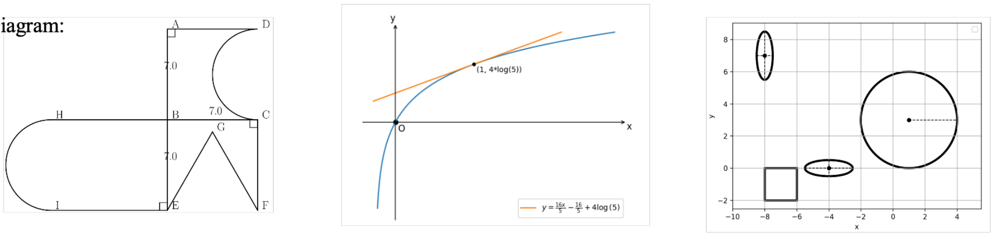

Caption:

A rectangle ABCD has a semicircle inscribed using CD as the diameter, and the base CD is removed. Connected to edge CB is a modified rectangle CBEF, ... Connected to edge EB is rectangle EBHI with a semicircle outside using HI as the diameter, and side HI is eliminated. The lengths of AB, CB, and EB are each 7.0 units.

In the coordinate system, there is a logarithmic function passing through the origin. Additionally, there is a line y = 16*x/5 - 16/5 + 4*log(5), which is tangent to the logarithmic curve at the point (1,4log(5)). The zero of the logarithmic function is at x=0, and the intersection point of the line with the y-axis is (0, -16/5 + 4*log(5)).

At the outset, A circle with a center at (1, 3) and radius 3 is present. Consequently, A rectangle originates from its lower left corner at (-8, -2) and has a height of 2 and a width of 2. Also, Located at (-8, 7), ..., At (-4, 0), there is an ellipse with dimensions: height 1 and width 3.

Figure 3: **MAVIS-Caption Dataset.** We showcase three diagram-caption pairs of plane geometry, function, and analytic geometry in MAVIS-Caption, generated by our developed data engine.

2.2 MAVIS-Caption

With our mathematical visual data engine, we first curate a diagram-caption dataset, MAVIS-Caption, as shown in Figure 3, aiming to benefit the diagram visual representations and cross-modal alignment.

Data Overview. As presented in Table 3 of the Appendix, the MAVIS-Caption dataset comprises 588K diagram-caption pairs. This includes 299K for plane geometry, 77K for analytic geometry, and 212K for function. The average word length of the captions is 61.48 words, reflecting their detailed descriptive nature. The overall vocabulary size is 149, indicating the diversity in language expression. We adopt different strategies to generate captions for three types of diagrams. It is important to note that GPT-4 (OpenAI, 2023b) is only utilized during the template creation stage; it is not used at any point during the automatic caption generation process.

Plane Geometry Caption. We follow the iterative geometric generation process to develop regulations for an accurate and detailed caption. We first prompt GPT-4 to create three sets of language templates: the descriptive content for fundamental shapes (e.g., *"A Triangle {} with two congruent sides {} and {}"*), the phrases to denote specific attributes (e.g., *"Angle {} measures {} degrees"*), and the conjunction to link two adjacent shapes (e.g., *"Attached to edge {} of shape {}, there is a {}"*). Then, based on various generation scenarios, we fill and merge these templates to acquire a coherent description of the geometric figure.

Function Caption. As function diagrams typically showcase a single curve, we directly utilize GPT-4 to generate templates describing various properties of functions, including expressions, domains, ranges, extreme points, and zero points. Each template is then filled based on specific cases, such as *"The expression of the function is* $y = -3x^3 - 2x^2 - 2x - 2$. *Within the range of x values* $[-3.0, 4.0]$, *zero points occur at* -0.83 *..."*.

Analytic Geometry Caption. We also employ GPT-4 to obtain two sets of language templates: the description of coordinates and attribute information for basic figures (e.g., *"The square with its base left corner at {} features sides of {} in length"*) and the spatial relation for nearby figures (e.g., *"On the bottom right of {}, there is a {}"*). The captions are then formulated by filling in the coordinates and selecting appropriate spatial relationship templates through coordinate comparison.

2.3 MAVIS-Instruct

Besides the diagram-caption data, we curate MAVIS-Instruct of extensive problem-solving data, which endows MLLMs with visual mathematical reasoning capabilities and serve as the basis for Direct Preference Optimization (DPO) (Rafailov et al., 2024), as shown in Figure 5.

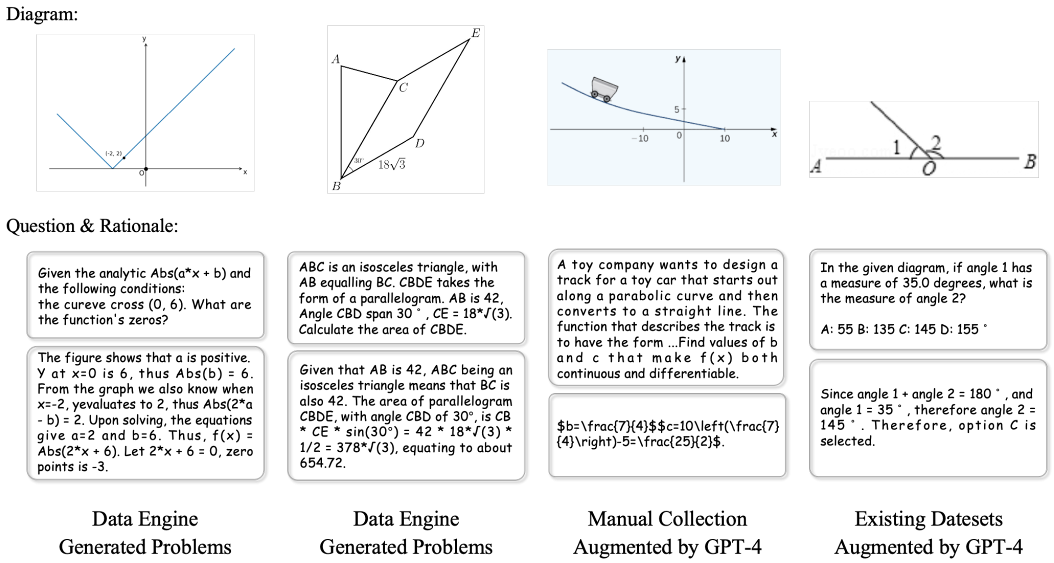

Given the analytic Abs(a*x + b) and the following conditions:
the cureve cross (0, 6). What are the function's zeros?

The figure shows that a is positive. Y at x=0 is 6, thus Abs(b) = 6. From the graph we also know when x=-2, yevaluates to 2, thus Abs(2*a - b) = 2. Upon solving, the equations give a=2 and b=6. Thus, f(x) = Abs(2*x + 6). Let 2*x + 6 = 0, zero points is -3.

ABC is an isosceles triangle, with AB equalling BC. CBDE takes the form of a parallelogram. AB is 42, Angle CBD span 30 ° , CE = 18*√(3). Calculate the area of CBDE.

Given that AB is 42, ABC being an isosceles triangle means that BC is also 42. The area of parallelogram CBDE, with angle CBD of 30°, is CB * CE * sin(30°) = 42 * 18*√(3) * 1/2 = 378*√(3), equating to about 654.72.

A toy company wants to design a track for a toy car that starts out along a parabolic curve and then converts to a straight line. The function that describes the track is to have the form ...Find values of b and c that make f(x) both continuous and differentiable.

`$b=\frac{7}{4}$$c=10\left(\frac{7}{4}\right)-5=\frac{25}{2}$.`

In the given diagram, if angle 1 has a measure of 35.0 degrees, what is the measure of angle 2?

A: 55 B: 135 C: 145 D: 155 °

Since angle 1 + angle 2 = 180 ° , and angle 1 = 35 ° , therefore angle 2 = 145 ° . Therefore, option C is selected.

Data Engine Generated Problems

Data Engine Generated Problems

Manual Collection Augmented by GPT-4

Existing Datesets Augmented by GPT-4

Figure 4: **MAVIS-Instruct Dataset.** We showcase the generated visual math problems from four sources within MAVIS-Instruct, which contain detailed rationales and minimized textual redundancy.

Data Overview. As illustrated in Table 4 of the Appendix, the MAVIS-Instruct dataset consists of a total of 834K visual math problems. Given that the proportion of analytic geometry problems is relatively small, we classify them with function problems for simplicity. Each problem in MAVIS-Instruct includes a CoT rationale providing step-by-step solutions, with an average answer length of 150 words. We have minimized textual redundancy in the questions, eliminating unnecessary contextual information, distracting conditions, and attributes readily observable from the diagrams. This reduction in text forces MLLMs to enhance their capability to extract essential content from visual inputs. MAVIS-Instruct is assembled from four distinct sources to ensure broad coverage.

Data Engine Generated Problems. Within our data engine, we manually craft rigorous regulations to produce visual math problems with accurate CoT annotations. Similar to caption generation, GPT API is not involved in the automatic synthesis process of questions, answers, and CoT rationales.

- **Plane Geometry Problems.** We initially prompt GPT-4 to compile a comprehensive set of mathematical formulas applicable to each basic shape (e.g., Pythagorean theorem for right triangles and area formula for circles). Then, for a geometric diagram, we randomly select a known condition within a shape as the final solution target, and systematically deduce backward to another condition, either within the same shape or an adjacent one, using a randomly selected mathematical formula. This deduced condition is then set as unknown, and we continue iterative backward deductions as necessary. The final condition, along with any conditions in the last step, are presented as initial attributes in the question. The rationales can be simply obtained by reversing this backward deduction process.
- **Function Problems.** As the properties of functions are predetermined, we utilize GPT-4 to generate diverse reasoning templates. These templates facilitate the solving of one function property based on other provided properties, thereby ensuring the generation of high-quality function rationales. The related function properties include analytical expression, function values, zeros, extremum points, monotonicity, derivatives, and integrals. To accurately reason these properties, the CoT annotation incorporates understanding of function types, solving the analytical expressions of equations, and interpreting function graphs.

Data Engine Captions Annotated by GPT-4. Given the detailed captions and diagrams generated by our data engine, we can prompt GPT-4V with these sufficient conditions to synthesis question-answering data and ensure its correctness. We first generate a new set of 17K diagram-caption pairs that do not overlap with the previous MAVIS-Caption, which avoids answer leakage within the detailed caption. Then, we prompt GPT-4V to generate 3 new problems with rationales, obtaining 51K data in total from the diagram-caption pairs.

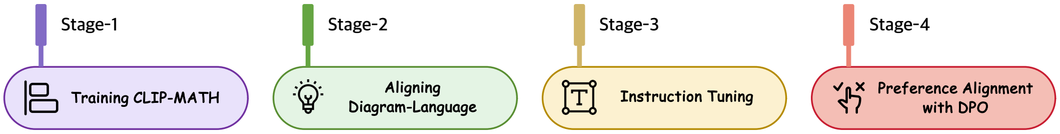

Figure 5: **Four-stage Training Pipeline of MAVIS.** With our curated MAVIS-Caption and MAVIS-Instruct, we adopt four progressive stages for training a mathematical visual specialist from scratch.

Manual Collection Augmented by GPT-4. To incorporate high-quality problems found in real-world contexts, we manually collect 4K math problems with diagrams from publicly available resources. Recognizing that these sources often lack detailed rationales and may contain redundant text, we initially utilize GPT-4V to annotate a detailed solving process and streamline the question text to reduce redundancy. Subsequently, for each collected instance, we input the question, rationale, and diagram into GPT-4 and employ customized few-shot prompts to generate 20 new problems per original, comprising 15 multiple-choice questions and 5 free-form questions. This process contributes a total of 83K problems to the dataset.

Existing Datasets Augmented by GPT-4. Given existing well-organized geometric datasets, we can also leverage them to expand MAVIS-Instruct. Referring to previous prompt designs, we augment the 8K training set from two dataset, Geometry-3K (Lu et al., 2021) and GeoQA+ (Chen et al., 2021b), into 80K visual problems with accompanying rationales, mapping each original problem to 10 new ones. Due to the scarcity of publicly available function data, we do not include function problems from this source.

3 Mathematical Visual Training

With the curated datasets, we devise a four-stage training pipeline for endowing MLLMs with mathematical visual capabilities. They respectively aim to mitigate the three deficiencies within existing MLLMs, i.e., diagram visual encoding, diagram-language alignment, and mathematical reasoning skills in visual contexts.

3.1 Stage 1: Training CLIP-Math

To enhance CLIP's (Radford et al., 2021) inadequate visual encoding of math diagrams, we utilize MAVIS-Caption to train a specialized CLIP-Math encoder. Specifically, we fine-tune a pre-trained CLIP-Base model following the conservative learning scheme. The math diagrams are fed into the learnable vision encoder, while the corresponding captions are processed by the text encoder, which remains frozen to provide reliable supervision. Via contrastive training, the model learns to adapt from its original natural image domain to mathematical contexts, increasing its focus on essential visual elements within diagrams, as demonstrated in Figure 1 (a). The optimized CLIP-Math encoder now delivers more precise and robust representations of math diagrams, establishing a solid foundation for the subsequent visual interpretation of LLMs.

3.2 Stage 2: Aligning Diagram-language

After acquiring the CLIP-Math encoder, we further integrate it with LLMs using MAVIS-Caption to boost cross-modal alignment between math diagrams and language embedding space. Using a simple two-layer MLP as the projection layer, we transform the visual encodings from CLIP-Math, and prepend them as a prefix to the LLM input. This process, guided by the diagram captioning task, enables the LLM to accurately recognize mathematical components and spatial arrangements. With the diagram-language alignment, LLMs are equipped with the interpretation capability in math diagrams, serving as an initial step toward deeper mathematical reasoning. In this stage, we freeze the CLIP-Math, and train the projection layer along with the LoRA-based (Hu et al., 2021) LLM.

3.3 Stage 3: Instruction Tuning

On top of that, we leverage MAVIS-Instruct to endow MLLMs with CoT reasoning and problem-solving capabilities in visual mathematics. The detailed rationales within each problem's solution

Table 1: **Evaluation on MathVerse's *testmini* Set with Six Problem Versions.** 'CoT-E' and 'Acc' denote the scores of CoT evaluation strategy and the scores of direct 'true or false' accuracy, respectively. '*' denotes previous mathematical visual specialists. The highest scores for closed-source and open-source MLLMs are marked in red and blue, respectively.

Model	LLM Size	All		Text Dominant		Text Lite		Vision Intensive		Vision Dominant		Vision Only	
		CoT-E	Acc	CoT-E	Acc	CoT-E	Acc	CoT-E	Acc	CoT-E	Acc	CoT-E	Acc
Baselines													
Random Chance	-	-	12.4	-	12.4	-	12.4	-	12.4	-	12.4	-	12.4
Human	-	-	64.9	-	71.2	-	70.9	-	61.4	-	68.3	-	66.7
LLMs													
ChatGPT	-	-	-	51.3	33.3	38.5	18.9	-	-	-	-	-	-
GPT-4	-	-	-	63.4	46.5	40.7	20.7	-	-	-	-	-	-
Closed-source MLLMs													
Qwen-VL-Plus	-	21.3	11.8	26.0	15.7	21.2	11.1	18.5	9.0	19.1	13.0	21.8	10.0
Gemini-Pro	-	35.3	23.5	39.8	26.3	34.7	23.5	32.0	23.0	36.8	22.3	33.3	22.2
Qwen-VL-Max	-	37.2	25.3	42.8	30.7	37.7	26.1	33.6	24.1	35.9	24.1	35.9	21.4
GPT-4V	-	54.4	39.4	63.1	54.7	56.6	41.4	51.4	34.9	50.8	34.4	50.3	31.6
Open-source MLLMs													
LLaMA-Adapter-V2	7B	5.8	5.7	7.8	6.2	6.3	5.9	6.2	6.1	4.5	4.2	4.4	6.1
ImageBind-LLM	7B	10.0	9.2	13.2	11.4	11.6	11.3	9.8	8.9	11.8	11.2	3.5	3.4
mPLUG-Owl2	7B	10.3	5.9	11.6	6.6	11.4	6.3	11.1	6.3	9.4	5.6	8.0	4.9
MiniGPT-v2	7B	10.9	11.0	13.2	12.1	12.7	12.0	11.1	13.1	11.3	10.3	6.4	7.4
LLaVA-1.5	7B	12.7	7.6	17.1	8.8	12.0	7.6	12.6	7.4	12.7	7.4	9.0	6.9
SPHINX-Plus	13B	14.0	12.2	16.3	13.9	12.8	11.6	12.9	11.6	14.7	13.5	13.2	10.4
G-LLaVA*	7B	15.7	16.6	22.2	20.9	20.4	20.7	16.5	17.2	12.7	14.6	6.6	9.4
LLaVA-NeXT	8B	17.2	15.6	21.6	19.4	19.7	15.2	17.6	16.8	14.9	15.2	12.1	11.3
ShareGPT4V	13B	17.4	13.1	21.8	16.2	20.6	16.2	18.6	15.5	16.2	13.8	9.7	3.7
SPHINX-MoE	8×7B	22.8	15.0	33.3	22.2	21.9	16.4	21.1	14.8	19.6	12.6	18.3	9.1
Math-LLaVA*	13B	24.1	19.0	34.2	21.2	22.7	19.8	21.1	20.2	20.3	17.6	22.2	16.4
InternLM-XC2.	7B	25.9	16.5	36.9	22.3	28.3	17.0	20.1	15.7	24.4	16.4	19.8	11.0
LLaVA-NeXT	110B	28.3	24.5	37.1	31.7	29.1	24.1	22.6	21.0	21.8	22.1	30.9	20.7
MAVIS-7B w/o DPO*	7B	33.7	27.5	42.5	41.4	36.3	29.1	33.3	27.4	29.3	24.9	27.1	14.6
MAVIS-7B*	7B	35.2	28.4	43.2	41.6	37.2	29.5	34.1	27.9	29.7	24.7	31.8	18.3

provide high-quality reasoning guidance for MLLMs, significantly enhancing their step-by-step CoT process. Furthermore, as we have minimized the redundancy within question texts during the construction process, such text-lite problem formats, referring to MathVerse (Zhang et al., 2024b), facilitate MLLMs to capture more essential information from the visual embeddings for problem-solving, rather than relying on shortcuts to only process the textual content. During this stage, we unfreeze both the projection layer and the LoRA-based (Hu et al., 2021) LLM to perform a thorough instruction-following tuning.

3.4 Stage 4: Preference Alignment with DPO

After the instruction tuning phase, the resulting model gains the capability for CoT reasoning on visual math problems. However, it may still produce inaccurate intermediate steps due to insufficient supervision for generating the best reasoning path. To address this, we further apply CoT preference alignment using the DPO (Rafailov et al., 2024) algorithm to further enhance the model's reasoning performance. Specifically, we adopt the instruction-tuned model to first infer CoT reasoning process on the 582K problems generated by data engine within MAVIS-Instruct. Then, we filter out the incorrect outputs (88K data) based on the final answer as the negative reasoning samples in DPO, and directly utilize the annotated CoT process as the positive samples. We only unfreeze the LoRA parameters for DPO training, and finally obtain our mathematical specialist, MAVIS-7B.

4 Experiment

We first detail our experimental settings in Section 4.1, and then discuss the quantitative on different benchmarks and qualitative examples in Sections 4.2 and 4.3, respectively. Please refer to the Appendix for more data details and ablation studies.

Table 2: **Evaluation on Six Mathematical Benchmarks.** ‘MMMU-Math’ denotes the math problems within the test set of MMMU. ‘GPS’, ‘ALG’, and ‘GEO’ denote geometry problem solving, algebraic, and geometry in MathVista’s *testmini* set. ‘S1’, ‘S2’, and ‘S3’ denote different problem steps in We-Math’s *testmini* set. ‘*’ denotes previous mathematical visual specialists. The highest scores for closed-source and open-source MLLMs are marked in red and blue, respectively.

Model	LLM Size	GeoQA	FunctionQA	MMMU-Math	MathVision	MathVista			We-Math		
						GPS	ALG	GEO	S1	S2	S3
Baselines											
Random Chance	-	17.1	-	21.6	7.2	24.1	25.8	22.7	-	-	-
Human	-	92.3	-	84.2	68.8	48.4	50.9	51.4	-	-	-
LLMs											
ChatGPT	-	-	-	-	9.7	31.7	32.4	33.0	-	-	-
GPT-4	-	-	-	30.6	13.1	31.7	33.5	32.2	-	-	-
Closed-source MLLMs											
Qwen-VL-Plus	-	-	-	-	10.7	38.5	39.1	39.3	-	-	-
Qwen-VL-Max	-	-	-	36.3	15.6	-	-	-	40.8	30.3	20.6
GPT-4V	-	-	-	48.4	22.8	50.5	53.0	51.0	65.5	49.2	38.2
Open-source MLLMs											
LLaMA-Adapter V2	7B	18.1	30.6	23.0	8.2	25.5	26.3	24.3	-	-	-
mPLUG-Owl2	7B	15.7	blue29.0	18.8	8.6	blue12.5	blue27.7	blue14.2	-	-	-
UniMath	-	50.0	-	-	-	-	-	-	-	-	-
LLaVA-1.5	13B	20.3	blue33.9	24.0	11.2	blue16.3	blue38.5	blue16.7	-	-	-
ShareGPT4V	13B	-	-	-	11.9	-	-	-	-	-	-
SPHINX-MoE	8×7B	-	33.9	-	14.2	31.2	31.7	30.5	-	-	-
G-LLaVA*	13B	67.0	blue24.2	blue27.6	blue1.3	blue36.1	blue24.6	blue33.1	32.4	30.1	32.7
Math-LLaVA*	13B	blue62.3	blue38.7	blue36.1	blue15.5	57.7	53.0	56.5	blue37.5	blue30.5	blue32.4
InternLM-XC2.	7B	blue66.4	blue38.7	30.1	14.5	63.0	56.6	62.3	47.0	33.1	33.0
LLaVA-NeXT	110B	-	-	-	-	-	-	-	53.7	36.9	31.5
MAVIS-7B w/o DPO*	7B	66.7	40.3	39.2	18.6	63.2	58.3	63.0	56.9	37.1	33.2
MAVIS-7B*	7B	68.3	50.0	42.4	19.2	64.1	59.2	63.2	57.2	37.9	34.6

4.1 Experimental Settings

Implementation Details. We adopt a CLIP ViT-L (Radford et al., 2021) as the pre-trained model to fine-tune our CLIP-Math, and utilize Mammoth2-7B (Yue et al., 2024) as the base LLM to construct MAVIS-7B. In the first stage, we fine-tune the CLIP for 10 epochs with a batch size 16 and an initial learning rate $2e^{-6}$. In the second stage, we train the diagram-language alignment for 1 epoch with a batch size 32 and an initial learning rate $2e^{-6}$, and adopt LoRA (Hu et al., 2021) with a rank 128. In the third and fourth stages, we adopt the same training settings as the second one.

Evaluation Schemes. We evaluate our model MAVIS-7B on several popular mathematical benchmarks, MathVerse (Zhang et al., 2024b), GeoQA (Chen et al., 2021c), FunctionQA (function problems in MathVista (Lu et al., 2023)), MMMU-Math (the math problems in MMMU (Yue et al., 2023a)), MathVision (Wang et al., 2024b), three mathematical categories in MathVista, and We-Math (Qiao et al., 2024). We compare a variety of existing MLLMs, including two mathematical visual specialist (Gao et al., 2023a; Shi et al., 2024), two LLMs (OpenAI, 2023a;b), and other general MLLMs (Bai et al., 2023b; Gao et al., 2023b; Ye et al., 2023b; Liu et al., 2023a; Chen et al., 2023b; Gao et al., 2024; Dong et al., 2024; Liu et al., 2024a; Chen et al., 2023a; Gao et al., 2024).

4.2 Quantitative Performance

As shown in Table 1 for the MathVerse benchmark, MAVIS-7B achieves the best overall scores in both CoT evaluation and accuracy among open-source MLLMs with only a 7B model size, and consistently surpasses the second-best method on different problem versions. Specifically, our model surpasses the powerful InternLM-XComposer2 (7B) (Dong et al., 2024) by +9.3% and ShareGPT4V (13B) (Chen et al., 2023b) by +17.8% CoT evaluation scores. Compared to other mathematical visual specialist, i.e., G-LLaVA (7B) (Gao et al., 2023a) and the concurrent Math-LLaVA (13B) (Shi et al., 2024), MAVIS-7B exhibits superior problem-solving capabilities with higher CoT evaluation scores of +19.5% and +11.1%, respectively. In addition, our model is also advantageous to the most powerful open-source MLLM series, LLaVA-NeXT (Li et al., 2024a), from 8B to 110B model sizes, demonstrating the math-specific proficiency of MAVIS-7B. Note that, the improvement brought by DPO (our fourth-stage training) is more apparent in CoT evaluation compared to the accuracy scores, indicating that the preference alignment learning can effectively boost the CoT reasoning capabilities.

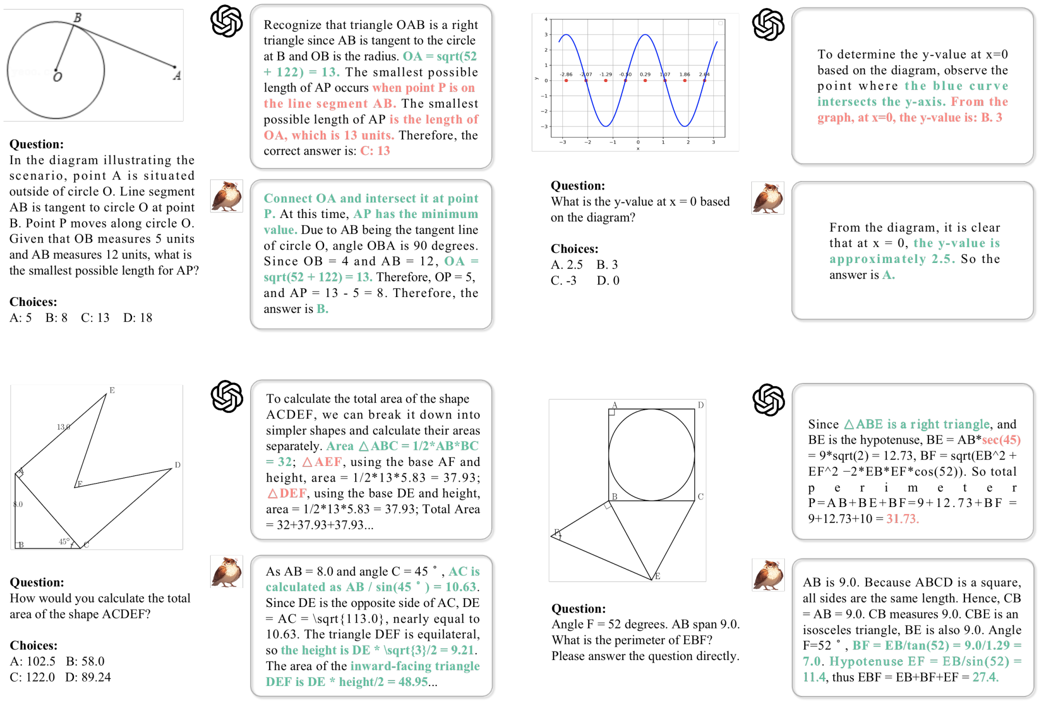

Question:
In the diagram illustrating the scenario, point A is situated outside of circle O. Line segment AB is tangent to circle O at point B. Point P moves along circle O. Given that OB measures 5 units and AB measures 12 units, what is the smallest possible length for AP?

Choices:
A: 5 B: 8 C: 13 D: 18

Recognize that triangle OAB is a right triangle since AB is tangent to the circle at B and OB is the radius. **OA = sqrt(52 + 122) = 13.** The smallest possible length of AP occurs **when point P is on the line segment AB.** The smallest possible length of AP **is the length of OA, which is 13 units.** Therefore, the correct answer is: **C: 13**

Connect OA and intersect it at point P. At this time, **AP has the minimum value.** Due to AB being the tangent line of circle O, angle OBA is 90 degrees. Since OB = 4 and AB = 12, **OA = sqrt(52 + 122) = 13.** Therefore, OP = 5, and AP = 13 - 5 = 8. Therefore, the answer is **B.**

Question:
What is the y-value at x = 0 based on the diagram?

Choices:
A. 2.5 B. 3
C. -3 D. 0

To determine the y-value at x=0 based on the diagram, observe the point where **the blue curve intersects the y-axis. From the graph, at x=0, the y-value is: B. 3**

From the diagram, it is clear that at x = 0, **the y-value is approximately 2.5.** So the answer is **A.**

Question:
How would you calculate the total area of the shape ACDEF?

Choices:
A: 102.5 B: 58.0
C: 122.0 D: 89.24

To calculate the total area of the shape ACDEF, we can break it down into simpler shapes and calculate their areas separately. **Area △ABC = 1/2*AB*BC = 32**; **△AEF**, using the base AF and height, area = 1/2*13*5.83 = 37.93; **△DEF**, using the base DE and height, area = 1/2*13*5.83 = 37.93; Total Area = 32+37.93+37.93...

As AB = 8.0 and angle C = 45 ° , **AC is calculated as AB / sin(45 °) = 10.63**. Since DE is the opposite side of AC, DE = AC = \sqrt{113.0}, nearly equal to 10.63. The triangle DEF is equilateral, so **the height is DE * \sqrt{3}/2 = 9.21**. The area of the **inward-facing triangle DEF is DE * height/2 = 48.95**...

Question:
Angle F = 52 degrees. AB span 9.0. What is the perimeter of EBF? Please answer the question directly.

Since **△ABE is a right triangle**, and BE is the hypotenuse, BE = AB***sec(45)** = 9*sqrt(2) = 12.73, BF = sqrt(EB^2 + EF^2 −2*EB*EF*cos(52)). So total perimeter P=AB+BE+BF=9+12.73+BF = 9+12.73+10 = **31.73.**

AB is 9.0. Because ABCD is a square, all sides are the same length. Hence, CB = AB = 9.0. CB measures 9.0. CBE is an isosceles triangle, BE is also 9.0. Angle F=52 ° , **BF = EB/tan(52) = 9.0/1.29 = 7.0**. **Hypotenuse EF = EB/sin(52) = 11.4**, thus EBF = EB+BF+EF = **27.4.**

Figure 6: **Problem-solving Comparison of MAVIS-7B and GPT-4V.**

Table 2 showcases the performance comparison on six other mathematical benchmarks, where our model still attains remarkable performance among other MLLMs. In detail, MAVIS-7B outperforms the closed-source Qwen-VL-Max (Bai et al., 2023a) by +6.1% in MMMU-Math, +3.6% in MathVision, and around +10% in three subsets of We-Math. Our model even exceeds GPT-4V (OpenAI, 2023b) in the three mathematical categories of MathVista, indicating our problem-solving and reasoning proficiency. We also observe that, the enhancement from DPO increases from 'S1' to 'S3' of We-Math, which well demonstrates its benefit on math problems with more intricate reasoning steps.

4.3 Qualitative Analysis

In Figure 6, we compare the mathematical problem-solving examples between MAVIS-7B and GPT-4V (OpenAI, 2023c). As presented, our model not only showcases better accuracy in understanding the geometric elements, function curves, and coordinate axes in mathematical diagrams, but also performs higher-quality step-by-step reasoning process for formula substitution and numerical calculation. This demonstrates the effectiveness of our four-stage training pipeline and automatic data engine for enhanced diagram understanding and CoT reasoning.

5 Conclusion

In this paper, we propose MAVIS, the first mathematical visual instruction tuning paradigm for MLLMs. We first introduce two high-quality datasets by a delicate data engine, MAVIS-Caption and MAVIS-Instruct, containing large-scale diagram-language and problem-solving data. Then, we customize a three-stage training framework to progressively train the math-specific vision encoder, the diagram-language alignment, and the mathematical reasoning capabilities of MLLMs. The obtained specialist model, MAVIS-7B, achieves superior performance across different mathematical visual benchmarks, demonstrating the potential to serve as a new standard for future research.

Acknowledgement

This project is funded in part by National Key R&D Program of China Project 2022ZD0161100, by the Centre for Perceptual and Interactive Intelligence (CPII) Ltd under the Innovation and Technology Commission (ITC)'s InnoHK, by NSFC-RGC Project N_CUHK498/24. Hongsheng Li is a PI of CPII under the InnoHK.

References

Jean-Baptiste Alayrac, Jeff Donahue, Pauline Luc, Antoine Miech, Iain Barr, Yana Hasson, Karel Lenc, Arthur Mensch, Katherine Millican, Malcolm Reynolds, et al. Flamingo: a visual language model for few-shot learning. *Advances in Neural Information Processing Systems*, 35:23716–23736, 2022.

Anas Awadalla, Irena Gao, Josh Gardner, Jack Hessel, Yusuf Hanafy, Wanrong Zhu, Kalyani Marathe, Yonatan Bitton, Samir Gadre, Shiori Sagawa, et al. Openflamingo: An open-source framework for training large autoregressive vision-language models. *arXiv preprint arXiv:2308.01390*, 2023.

Jinze Bai, Shuai Bai, Shusheng Yang, Shijie Wang, Sinan Tan, Peng Wang, Junyang Lin, Chang Zhou, and Jingren Zhou. Qwen-vl: A frontier large vision-language model with versatile abilities. *ArXiv*, abs/2308.12966, 2023a.

Jinze Bai, Shuai Bai, Shusheng Yang, Shijie Wang, Sinan Tan, Peng Wang, Junyang Lin, Chang Zhou, and Jingren Zhou. Qwen-vl: A versatile vision-language model for understanding, localization, text reading, and beyond. *arXiv preprint arXiv:2308.12966*, 2023b.

Tom Brown, Benjamin Mann, Nick Ryder, Melanie Subbiah, Jared D Kaplan, Prafulla Dhariwal, Arvind Neelakantan, Pranav Shyam, Girish Sastry, Amanda Askell, et al. Language models are few-shot learners. In *Advances in neural information processing systems*, pp. 1877–1901, 2020.

Jiaqi Chen, Jianheng Tang, Jinghui Qin, Xiaodan Liang, Lingbo Liu, Eric Xing, and Liang Lin. GeoQA: A geometric question answering benchmark towards multimodal numerical reasoning. In Chengqing Zong, Fei Xia, Wenjie Li, and Roberto Navigli (eds.), *Findings of the Association for Computational Linguistics: ACL-IJCNLP 2021*, pp. 513–523, Online, August 2021a. Association for Computational Linguistics. doi: 10.18653/v1/2021.findings-acl.46. URL https://aclanthology.org/2021.findings-acl.46.

Jiaqi Chen, Jianheng Tang, Jinghui Qin, Xiaodan Liang, Lingbo Liu, Eric P. Xing, and Liang Lin. Geoqa: A geometric question answering benchmark towards multimodal numerical reasoning. *ArXiv*, abs/2105.14517, 2021b. URL https://api.semanticscholar.org/CorpusID:235253782.

Jiaqi Chen, Jianheng Tang, Jinghui Qin, Xiaodan Liang, Lingbo Liu, Eric P Xing, and Liang Lin. Geoqa: A geometric question answering benchmark towards multimodal numerical reasoning. *arXiv preprint arXiv:2105.14517*, 2021c.

Jiaqi Chen, Tong Li, Jinghui Qin, Pan Lu, Liang Lin, Chongyu Chen, and Xiaodan Liang. Unigeo: Unifying geometry logical reasoning via reformulating mathematical expression. *ArXiv*, abs/2212.02746, 2022.

Jun Chen, Deyao Zhu1 Xiaoqian Shen1 Xiang Li, Zechun Liu2 Pengchuan Zhang, Raghuraman Krishnamoorthi2 Vikas Chandra2 Yunyang Xiong, and Mohamed Elhoseiny. Minigpt-v2: Large language model as a unified interface for vision-language multi-task learning. *arXiv preprint arXiv:2310.09478*, 2023a.

Lin Chen, Jinsong Li, Xiao wen Dong, Pan Zhang, Conghui He, Jiaqi Wang, Feng Zhao, and Dahua Lin. Sharegpt4v: Improving large multi-modal models with better captions. *ArXiv*, abs/2311.12793, 2023b. URL https://api.semanticscholar.org/CorpusID:265308687.

Zhe Chen, Weiyun Wang, Hao Tian, Shenglong Ye, Zhangwei Gao, Erfei Cui, Wenwen Tong, Kongzhi Hu, Jiapeng Luo, Zheng Ma, et al. How far are we to gpt-4v? closing the gap to commercial multimodal models with open-source suites. *arXiv preprint arXiv:2404.16821*, 2024.

Wei-Lin Chiang, Zhuohan Li, Zi Lin, Ying Sheng, Zhanghao Wu, Hao Zhang, Lianmin Zheng, Siyuan Zhuang, Yonghao Zhuang, Joseph E. Gonzalez, Ion Stoica, and Eric P. Xing. Vicuna: An open-source chatbot impressing gpt-4 with 90%* chatgpt quality. https://lmsys.org/blog/2023-03-30-vicuna/, March 2023.

Xiaoyi Dong, Pan Zhang, Yuhang Zang, Yuhang Cao, Bin Wang, Linke Ouyang, Xilin Wei, Songyang Zhang, Haodong Duan, Maosong Cao, et al. Internlm-xcomposer2: Mastering free-form text-image composition and comprehension in vision-language large model. *arXiv preprint arXiv:2401.16420*, 2024.

Chaoyou Fu, Yuhan Dai, Yondong Luo, Lei Li, Shuhuai Ren, Renrui Zhang, Zihan Wang, Chenyu Zhou, Yunhang Shen, Mengdan Zhang, et al. Video-mme: The first-ever comprehensive evaluation benchmark of multi-modal llms in video analysis. *arXiv preprint arXiv:2405.21075*, 2024.

Jiahui Gao, Renjie Pi, Jipeng Zhang, Jiacheng Ye, Wanjun Zhong, Yufei Wang, Lanqing Hong, Jianhua Han, Hang Xu, Zhenguo Li, et al. G-llava: Solving geometric problem with multi-modal large language model. *arXiv preprint arXiv:2312.11370*, 2023a.

Peng Gao, Jiaming Han, Renrui Zhang, Ziyi Lin, Shijie Geng, Aojun Zhou, Wei Zhang, Pan Lu, Conghui He, Xiangyu Yue, Hongsheng Li, and Yu Qiao. Llama-adapter v2: Parameter-efficient visual instruction model. *arXiv preprint arXiv:2304.15010*, 2023b.

Peng Gao, Renrui Zhang, Chris Liu, Longtian Qiu, Siyuan Huang, Weifeng Lin, Shitian Zhao, Shijie Geng, Ziyi Lin, Peng Jin, et al. Sphinx-x: Scaling data and parameters for a family of multi-modal large language models. *arXiv preprint arXiv:2402.05935*, 2024.

Google Gemini Team. Gemini: a family of highly capable multimodal models. *arXiv preprint arXiv:2312.11805*, 2023.

Zhibin Gou, Zhihong Shao, Yeyun Gong, Yujiu Yang, Minlie Huang, Nan Duan, Weizhu Chen, et al. Tora: A tool-integrated reasoning agent for mathematical problem solving. *arXiv preprint arXiv:2309.17452*, 2023.

Ziyu Guo, Renrui Zhang, Xiangyang Zhu, Yiwen Tang, Xianzheng Ma, Jiaming Han, Kexin Chen, Peng Gao, Xianzhi Li, Hongsheng Li, et al. Point-bind & point-llm: Aligning point cloud with multi-modality for 3d understanding, generation, and instruction following. *arXiv preprint arXiv:2309.00615*, 2023.

Ziyu Guo*, Renrui Zhang*#, Xiangyang Zhu, Chengzhuo Tong, Peng Gao, Chunyuan Li, and Pheng-Ann Heng. Sam2point: Segment any 3d as videos in zero-shot and promptable manners. *arXiv preprint arXiv:2408.16768*, 2024.

Ziyu Guo, Renrui Zhang, Chengzhuo Tong, Zhizheng Zhao, Peng Gao, Hongsheng Li, and Pheng-Ann Heng. Can we generate images with cot? let's verify and reinforce image generation step by step. *arXiv preprint arXiv:2501.13926*, 2025.

Jiaming Han, Renrui Zhang, Wenqi Shao, Peng Gao, Peng Xu, Han Xiao, Kaipeng Zhang, Chris Liu, Song Wen, Ziyu Guo, et al. Imagebind-llm: Multi-modality instruction tuning. *arXiv preprint arXiv:2309.03905*, 2023.

Edward J Hu, Yelong Shen, Phillip Wallis, Zeyuan Allen-Zhu, Yuanzhi Li, Shean Wang, Lu Wang, and Weizhu Chen. Lora: Low-rank adaptation of large language models. *arXiv preprint arXiv:2106.09685*, 2021.

Yueru Jia, Jiaming Liu, Sixiang Chen, Chenyang Gu, Zhilue Wang, Longzan Luo, Lily Lee, Pengwei Wang, Zhongyuan Wang, Renrui Zhang, et al. Lift3d foundation policy: Lifting 2d large-scale pretrained models for robust 3d robotic manipulation. *arXiv preprint arXiv:2411.18623*, 2024.

Albert Q. Jiang, Alexandre Sablayrolles, Antoine Roux, Arthur Mensch, Blanche Savary, Chris Bamford, Devendra Singh Chaplot, Diego de Las Casas, Emma Bou Hanna, Florian Bressand, Gianna Lengyel, Guillaume Bour, Guillaume Lample, Lélio Renard Lavaud, Lucile Saulnier, Marie-Anne Lachaux, Pierre Stock, Sandeep Subramanian, Sophia Yang, Szymon Antoniak, Teven Le Scao, Théophile Gervet, Thibaut Lavril, Thomas Wang, Timothée Lacroix, and William El Sayed. Mixtral of experts. *Arxiv 2401.04088*, 2024.

Dongzhi Jiang, Renrui Zhang, Ziyu Guo, Yanwei Li, Yu Qi, Xinyan Chen, Liuhui Wang, Jianhan Jin, Claire Guo, Shen Yan, et al. Mme-cot: Benchmarking chain-of-thought in large multimodal models for reasoning quality, robustness, and efficiency. *arXiv preprint arXiv:2502.09621*, 2025.

Bu Jin, Yupeng Zheng, Pengfei Li, Weize Li, Yuhang Zheng, Sujie Hu, Xinyu Liu, Jinwei Zhu, Zhijie Yan, Haiyang Sun, et al. Tod3cap: Towards 3d dense captioning in outdoor scenes. *arXiv preprint arXiv:2403.19589*, 2024.

Mehran Kazemi, Hamidreza Alvari, Ankit Anand, Jialin Wu, Xi Chen, and Radu Soricut. Geomverse: A systematic evaluation of large models for geometric reasoning. *arXiv preprint arXiv:2312.12241*, 2023.

Bo Li, Kaichen Zhang, Hao Zhang, Dong Guo, Renrui Zhang, Feng Li, Yuanhan Zhang, Ziwei Liu, and Chunyuan Li. Llava-next: Stronger llms supercharge multimodal capabilities in the wild, May 2024a. URL https://llava-vl.github.io/blog/2024-05-10-llava-next-stronger-llms/.

Feng Li, Renrui Zhang, Hao Zhang, Yuanhan Zhang, Bo Li, Wei Li, Zejun Ma, and Chunyuan Li. Llava-next: Tackling multi-image, video, and 3d in large multimodal models, June 2024b. URL https://llava-vl.github.io/blog/2024-06-16-llava-next-interleave/.

Feng Li, Renrui Zhang, Hao Zhang, Yuanhan Zhang, Bo Li, Wei Li, Zejun Ma, and Chunyuan Li. Llava-next-interleave: Tackling multi-image, video, and 3d in large multimodal models, 2024c. URL https://arxiv.org/abs/2407.07895.

Junnan Li, Dongxu Li, Caiming Xiong, and Steven Hoi. Blip: Bootstrapping language-image pre-training for unified vision-language understanding and generation. In *International Conference on Machine Learning*, pp. 12888–12900. PMLR, 2022.

KunChang Li, Yinan He, Yi Wang, Yizhuo Li, Wenhai Wang, Ping Luo, Yali Wang, Limin Wang, and Yu Qiao. Videochat: Chat-centric video understanding. *arXiv preprint arXiv:2305.06355*, 2023a.

Xiaoqi Li, Mingxu Zhang, Yiran Geng, Haoran Geng, Yuxing Long, Yan Shen, Renrui Zhang, Jiaming Liu, and Hao Dong. Manipllm: Embodied multimodal large language model for object-centric robotic manipulation. *arXiv preprint arXiv:2312.16217*, 2023b.

Zhenwen Liang, Tianyu Yang, Jipeng Zhang, and Xiangliang Zhang. Unimath: A foundational and multimodal mathematical reasoner. In *EMNLP*, 2023.

Weifeng Lin, Xinyu Wei, Ruichuan An, Peng Gao, Bocheng Zou, Yulin Luo, Siyuan Huang, Shanghang Zhang, and Hongsheng Li. Draw-and-understand: Leveraging visual prompts to enable mllms to comprehend what you want, 2025. URL https://arxiv.org/abs/2403.20271.

Ziyi Lin, Chris Liu, Renrui Zhang, Peng Gao, Longtian Qiu, Han Xiao, Han Qiu, Chen Lin, Wenqi Shao, Keqin Chen, et al. Sphinx: The joint mixing of weights, tasks, and visual embeddings for multi-modal large language models. *arXiv preprint arXiv:2311.07575*, 2023.

Haotian Liu, Chunyuan Li, Yuheng Li, and Yong Jae Lee. Improved baselines with visual instruction tuning, 2023a.

Haotian Liu, Chunyuan Li, Qingyang Wu, and Yong Jae Lee. Visual instruction tuning. In *NeurIPS*, 2023b.

Haotian Liu, Chunyuan Li, Yuheng Li, Bo Li, Yuanhan Zhang, Sheng Shen, and Yong Jae Lee. Llava-next: Improved reasoning, ocr, and world knowledge, January 2024a. URL https://llava-vl.github.io/blog/2024-01-30-llava-next/.

Jiaming Liu, Chenxuan Li, Guanqun Wang, Lily Lee, Kaichen Zhou, Sixiang Chen, Chuyan Xiong, Jiaxin Ge, Renrui Zhang, and Shanghang Zhang. Self-corrected multimodal large language model for end-to-end robot manipulation. *arXiv preprint arXiv:2405.17418*, 2024b.

Jiaming Liu, Mengzhen Liu, Zhenyu Wang, Lily Lee, Kaichen Zhou, Pengju An, Senqiao Yang, Renrui Zhang, Yandong Guo, and Shanghang Zhang. Robomamba: Multimodal state space model for efficient robot reasoning and manipulation. *NeurIPS 2024*, 2024c.

Pan Lu, Ran Gong, Shibiao Jiang, Liang Qiu, Siyuan Huang, Xiaodan Liang, and Song-Chun Zhu. Inter-gps: Interpretable geometry problem solving with formal language and symbolic reasoning. *arXiv preprint arXiv:2105.04165*, 2021.

Pan Lu, Hritik Bansal, Tony Xia, Jiacheng Liu, Chun yue Li, Hannaneh Hajishirzi, Hao Cheng, Kai-Wei Chang, Michel Galley, and Jianfeng Gao. Mathvista: Evaluating math reasoning in visual contexts with gpt-4v, bard, and other large multimodal models. *ArXiv*, abs/2310.02255, 2023.

Maxwell Nye, Anders Johan Andreassen, Guy Gur-Ari, Henryk Michalewski, Jacob Austin, David Bieber, David Dohan, Aitor Lewkowycz, Maarten Bosma, David Luan, et al. Show your work: Scratchpads for intermediate computation with language models. *arXiv preprint arXiv:2112.00114*, 2021.

OpenAI. Chatgpt. https://chat.openai.com, 2023a.

OpenAI. Gpt-4 technical report. *ArXiv*, abs/2303.08774, 2023b.

OpenAI. GPT-4V(ision) system card, 2023c. URL https://openai.com/research/gpt-4v-system-card.

Tianshuo Peng, Mingsheng Li, Hongbin Zhou, Renqiu Xia, Renrui Zhang, Lei Bai, Song Mao, Bin Wang, Conghui He, Aojun Zhou, et al. Chimera: Improving generalist model with domain-specific experts. *arXiv preprint arXiv:2412.05983*, 2024.

Runqi Qiao, Qiuna Tan, Guanting Dong, Minhui Wu, Chong Sun, Xiaoshuai Song, Zhuoma GongQue, Shanglin Lei, Zhe Wei, Miaoxuan Zhang, et al. We-math: Does your large multimodal model achieve human-like mathematical reasoning? *arXiv preprint arXiv:2407.01284*, 2024.

Alec Radford, Jong Wook Kim, Chris Hallacy, Aditya Ramesh, Gabriel Goh, Sandhini Agarwal, Girish Sastry, Amanda Askell, Pamela Mishkin, Jack Clark, Gretchen Krueger, and Ilya Sutskever. Learning transferable visual models from natural language supervision. In *International Conference on Machine Learning*, 2021. URL https://api.semanticscholar.org/CorpusID:231591445.

Rafael Rafailov, Archit Sharma, Eric Mitchell, Stefano Ermon, Christopher D. Manning, and Chelsea Finn. Direct preference optimization: Your language model is secretly a reward model, 2024. URL https://arxiv.org/abs/2305.18290.

Wenhao Shi, Zhiqiang Hu, Yi Bin, Junhua Liu, Yang Yang, See-Kiong Ng, Lidong Bing, and Roy Ka-Wei Lee. Math-llava: Bootstrapping mathematical reasoning for multimodal large language models. *arXiv preprint arXiv:2406.17294*, 2024.

Chang Shu, Baian Chen, Fangyu Liu, Zihao Fu, Ehsan Shareghi, and Nigel Collier. Visual med-alpaca: A parameter-efficient biomedical llm with visual capabilities, 2023.

Karan Singhal, Tao Tu, Juraj Gottweis, Rory Sayres, Ellery Wulczyn, Le Hou, Kevin Clark, Stephen Pfohl, Heather Cole-Lewis, Darlene Neal, et al. Towards expert-level medical question answering with large language models. *arXiv preprint arXiv:2305.09617*, 2023.

Yixuan Su, Tian Lan, Huayang Li, Jialu Xu, Yan Wang, and Deng Cai. Pandagpt: One model to instruction-follow them all. *arXiv preprint arXiv:2305.16355*, 2023.

Yiwen Tang, Zoey Guo, Zhuhao Wang, Ray Zhang, Qizhi Chen, Junli Liu, Delin Qu, Zhigang Wang, Dong Wang, Xuelong Li, et al. Exploring the potential of encoder-free architectures in 3d lmms. *arXiv preprint arXiv:2502.09620*, 2025.

InternLM Team. Internlm: A multilingual language model with progressively enhanced capabilities, 2023.

Hugo Touvron, Thibaut Lavril, Gautier Izacard, Xavier Martinet, Marie-Anne Lachaux, Timothée Lacroix, Baptiste Rozière, Naman Goyal, Eric Hambro, Faisal Azhar, et al. Llama: Open and efficient foundation language models. *arXiv preprint arXiv:2302.13971*, 2023a.

Hugo Touvron, Louis Martin, Kevin Stone, Peter Albert, Amjad Almahairi, Yasmine Babaei, Nikolay Bashlykov, Soumya Batra, Prajjwal Bhargava, Shruti Bhosale, et al. Llama 2: Open foundation and fine-tuned chat models. *arXiv preprint arXiv:2307.09288*, 2023b.

Guanqun Wang, Xinyu Wei, Jiaming Liu, Ray Zhang, Yichi Zhang, Kevin Zhang, Maurice Chong, and Shanghang Zhang. Mr-mllm: Mutual reinforcement of multimodal comprehension and vision perception, 2024a. URL https://arxiv.org/abs/2406.15768.

Ke Wang, Junting Pan, Weikang Shi, Zimu Lu, Mingjie Zhan, and Hongsheng Li. Measuring multimodal mathematical reasoning with math-vision dataset. *arXiv preprint arXiv:2402.14804*, 2024b.

Ke Wang, Houxing Ren, Aojun Zhou, Zimu Lu, Sichun Luo, Weikang Shi, Renrui Zhang, Linqi Song, Mingjie Zhan, and Hongsheng Li. Mathcoder: Seamless code integration in LLMs for enhanced mathematical reasoning. In *The Twelfth International Conference on Learning Representations*, 2024c. URL https://openreview.net/forum?id=z8TW0ttBPp.

Jason Wei, Xuezhi Wang, Dale Schuurmans, Maarten Bosma, Fei Xia, Ed Chi, Quoc V Le, Denny Zhou, et al. Chain-of-thought prompting elicits reasoning in large language models. *Advances in Neural Information Processing Systems*, 35:24824–24837, 2022.

Runsen Xu, Xiaolong Wang, Tai Wang, Yilun Chen, Jiangmiao Pang, and Dahua Lin. Pointllm: Empowering large language models to understand point clouds. *arXiv preprint arXiv:2308.16911*, 2023.

Senqiao Yang, Jiaming Liu, Ray Zhang, Mingjie Pan, Zoey Guo, Xiaoqi Li, Zehui Chen, Peng Gao, Yandong Guo, and Shanghang Zhang. Lidar-llm: Exploring the potential of large language models for 3d lidar understanding. *arXiv preprint arXiv:2312.14074*, 2023.

Qinghao Ye, Haiyang Xu, Guohai Xu, Jiabo Ye, Ming Yan, Yiyang Zhou, Junyang Wang, Anwen Hu, Pengcheng Shi, Yaya Shi, Chaoya Jiang, Chenliang Li, Yuanhong Xu, Hehong Chen, Junfeng Tian, Qi Qian, Ji Zhang, and Fei Huang. mplug-owl: Modularization empowers large language models with multimodality, 2023a.

Qinghao Ye, Haiyang Xu, Jiabo Ye, Ming Yan, Anwen Hu, Haowei Liu, Qi Qian, Ji Zhang, Fei Huang, and Jingren Zhou. mplug-owl2: Revolutionizing multi-modal large language model with modality collaboration, 2023b.

Longhui Yu, Weisen Jiang, Han Shi, Jincheng Yu, Zhengying Liu, Yu Zhang, James T Kwok, Zhenguo Li, Adrian Weller, and Weiyang Liu. Metamath: Bootstrap your own mathematical questions for large language models. *arXiv preprint arXiv:2309.12284*, 2023.

Xiang Yue, Yuansheng Ni, Kai Zhang, Tianyu Zheng, Ruoqi Liu, Ge Zhang, Samuel Stevens, Dongfu Jiang, Weiming Ren, Yuxuan Sun, Cong Wei, Botao Yu, Ruibin Yuan, Renliang Sun, Ming Yin, Boyuan Zheng, Zhenzhu Yang, Yibo Liu, Wenhao Huang, Huan Sun, Yu Su, and Wenhu Chen. Mmmu: A massive multi-discipline multimodal understanding and reasoning benchmark for expert agi. *arXiv preprint arXiv:2311.16502*, 2023a.

Xiang Yue, Xingwei Qu, Ge Zhang, Yao Fu, Wenhao Huang, Huan Sun, Yu Su, and Wenhu Chen. Mammoth: Building math generalist models through hybrid instruction tuning. *arXiv preprint arXiv:2309.05653*, 2023b.

Xiang Yue, Tuney Zheng, Ge Zhang, and Wenhu Chen. Mammoth2: Scaling instructions from the web. *arXiv preprint arXiv:2405.03548*, 2024.

Renrui Zhang, Jiaming Han, Aojun Zhou, Xiangfei Hu, Shilin Yan, Pan Lu, Hongsheng Li, Peng Gao, and Yu Qiao. LLaMA-adapter: Efficient fine-tuning of large language models with zero-initialized attention. In *The Twelfth International Conference on Learning Representations*, 2024a. URL https://openreview.net/forum?id=d4UiXAHN2W.

Renrui Zhang, Dongzhi Jiang, Yichi Zhang, Haokun Lin, Ziyu Guo, Pengshuo Qiu, Aojun Zhou, Pan Lu, Kai-Wei Chang, Peng Gao, et al. Mathverse: Does your multi-modal llm truly see the diagrams in visual math problems? *arXiv preprint arXiv:2403.14624*, 2024b.

Aojun Zhou, Ke Wang, Zimu Lu, Weikang Shi, Sichun Luo, Zipeng Qin, Shaoqing Lu, Anya Jia, Linqi Song, Mingjie Zhan, et al. Solving challenging math word problems using gpt-4 code interpreter with code-based self-verification. *arXiv preprint arXiv:2308.07921*, 2023.

A Appendix

A.1 Related Work

Visual Instruction Tuning. The advancement of large language models (LLMs) (Brown et al., 2020; Jiang et al., 2024; Touvron et al., 2023b; Chiang et al., 2023) with instruction tuning has significantly enhanced zero-shot capabilities across a range of tasks. Drawing inspiration from this, LLaMA-Adapter series (Zhang et al., 2024a; Gao et al., 2023b; Han et al., 2023) propose a zero-initialized attention mechanism to align frozen vision encoders (Radford et al., 2021) with LLaMA (Touvron et al., 2023a) for multi-modal learning. LLaVA series (Liu et al., 2023b;a) employ a linear projector for vision-language alignment, establishing visual instruction tuning as a standard training approach in the multi-modal field. Flamingo (Alayrac et al., 2022) and OpenFlamingo (Awadalla et al., 2023) have honed visual representation by integrating a cross-attention resampler with vision encoders. SPHINX series (Gao et al., 2024; Lin et al., 2023; 2025) and MR-MLLM (Wang et al., 2024a) utilize a blend of visual encoders to make the LLM cognizant of various image aspects. InternVL series (Chen et al., 2024; Dong et al., 2024; Team, 2023) employ a large vision encoder and Q-Former (Li et al., 2022) to incorporate high-quality visual information through a multi-stage training methodology. LLaVA-NexT (Liu et al., 2024a; Li et al., 2024a;b) further introduces the 'AnyRes' technique to manage images at any given resolution, and LLaVA-NexT-Interleave (Li et al., 2024c) extends the scope widely to interleave multi-image settings. There are also recent efforts to apply visual instruction tuning to 3D (Guo et al., 2023; Xu et al., 2023; Guo* et al., 2024; Tang et al., 2025), video (Li et al., 2023a; Fu et al., 2024), reasoning Guo et al. (2025); Jiang et al. (2025); Peng et al. (2024), and robotics Jia et al. (2024); Liu et al. (2024c) scenarios. Despite the impressive strides made in both model capability and training efficiency by multi-modal large language models (MLLMs) through visual instruction tuning, there is currently no MLLM specifically designed for mathematical problem-solving, nor a substantial dataset available for such purposes in the open-source community. In this paper, we mitigate the issue by proposing MAVIS with high-quality mathematical visual datasets and training paradigms.

Mathematics in Large Models. Recent research has predominantly concentrated on text-only mathematical problem-solving using LLMs. MAmmoTH (Yue et al., 2023b; 2024) have compiled extensive collections of mathematical problems, training LLMs using the reasoning processes described in solutions. MetaMATH (Yu et al., 2023) has expanded upon this by rewriting existing problems to create a larger dataset. MathCoder (Wang et al., 2024c) and ToRA (Gou et al., 2023) introduced a tools agent approach, employing Python code and symbolic resolvers during the training phase, significantly outperforming traditional models that rely on text-only mathematical reasoning. However, in the multi-modal field, despite the introduction of several datasets such as Geometry3K (Lu et al., 2021), GeoQA (Chen et al., 2021b), UniGeo (Chen et al., 2022), UniMath (Liang et al., 2023), and GeomVerse (Kazemi et al., 2023), aiming at enhancing the performance of MLLMs in solving graphical mathematical problems, these datasets are quite limited in scale and domain. Based on these datasets, G-LLaVA (Gao et al., 2023a) has developed superior capabilities for understanding graphical geometries but struggles with mathematical problems in other domains. The comprehensive benchmark MathVerse (Zhang et al., 2024b) has also highlighted the existing MLLMs' unsatisfactory capacity for encoding visual diagrams in diverse mathematical domains. Therefore, there is a pressing need for the development of more robust encoders for mathematical images and the tuning of MLLMs with mathematical visual instructions, for which we propose MAVIS to address the challenges.

A.2 Human Evaluation of MAVIS-Instruct

To assess the dataset's coverage, validity, and quality, human verification is employed. The creation process of our MAVIS-Instruct dataset can be broadly categorized into two approaches:

- **GPT-generated:** This method leverages GPT-4 to generate new problems (including questions, rationales, and answers) based on existing problems with diagrams. While this approach produces fluent, human-like sentences, it may be influenced by the inherent capabilities and occasional instability of GPT-4V.
- **Data Engine:** As the main source of our mathematical visual data, this method utilizes the custom automatic data engine to generate new problems (including diagrams, questions,

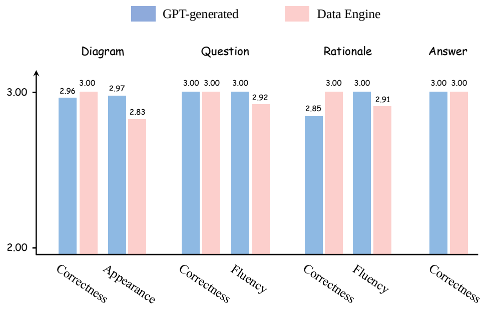

Figure 7: **Human Evaluation Results** on 200 randomly sampled problems in MAVIS-Instruct, 100 GPT-generated and 100 Data Engine. We set three levels (1, 2, and 3) for each metric, and report average scores.

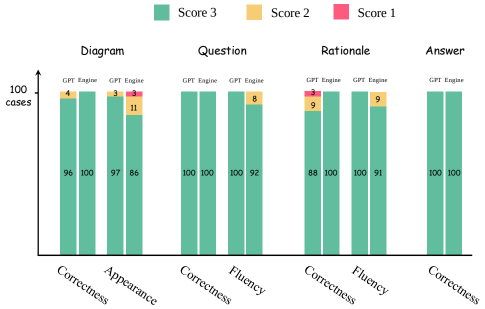

Figure 8: **Human Evaluation Statistics** on 200 randomly sampled problems in MAVIS-Instruct, 100 GPT-generated and 100 Data Engine. We count the numbers of three score levels (1, 2, and 3) for each metric.

rationales, and answers), without relying on GPT models. It guarantees 100% correctness due to the use of rigorous templates, though it may occasionally exhibit rigid expressions.

Specifically, we evaluate four aspects(Diagram, Question, Rationale and Answer) of each problem using seven metrics. Each metric is scored on a scale of 1 to 3, where 1 denotes *poor*, 2 denotes *moderate*, and 3 denotes *good*. The human evaluation results are shown in Figure 7 and score statistics are shown in Figure 8. In addition, we also showcase some specific examples in Figure 9 and Figure 10. We analyze each aspect as follows:

- **Diagram:** The diagrams in GPT-generated problems are directly collected from existing sources with rigorous human filtering, ensuring high quality, resulting in scores close to 3. In contrast, for rule-based problems, the diagrams are drawn accurately using Python code driven by our data engine, which guarantees correctness. However, these diagrams may lack alignment with human aesthetic preferences, as indicated by 3% of them receiving an appearance score of 1.

- **Question:** Regarding the questions, both GPT-generated and rule-based problems display a high degree of accuracy in aligning with the diagram elements. This is attributed to the well-crafted prompts used with GPT-4 and the meticulous template design of the data engine. Nevertheless, rule-based questions may occasionally exhibit minor fluency issues, as they lack human refinement.

- **Rationale:** In terms of the rationales, most instances feature a precise and detailed chain-of-thought (CoT) reasoning process. However, in a few cases (3% receiving an accuracy score of 1), some GPT-generated rationales contain minor reasoning or calculation errors, which are inherent to GPT-4's limitations in problem-solving. These errors usually affect only one or two steps and do not compromise the overall logic. Conversely, the rule-based rationales are highly accurate due to the carefully designed data engine, although there is still room for improvement in language fluency.

- **Answer:** The answers in both methods achieve high correctness scores. For GPT-generated problems, we prompt GPT-4 to identify a known condition from the original problems as the answer. Similarly, for rule-based problems, we randomly select a known attribute from the generated diagrams to serve as the answer.

Overall, the randomly sampled instances show that our dataset exhibits good question quality and answer accuracy.

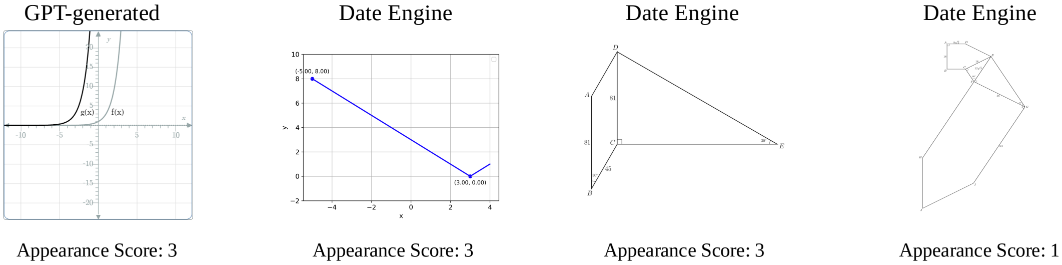

Figure 9: **Diagram Examples in MAVIS-Instruct.** The first three diagrams showcase superior correctness and appearance, while a small portion of Data Engine generated diagrams (3%) are not aligned with human preference, e.g., the fourth diagram.

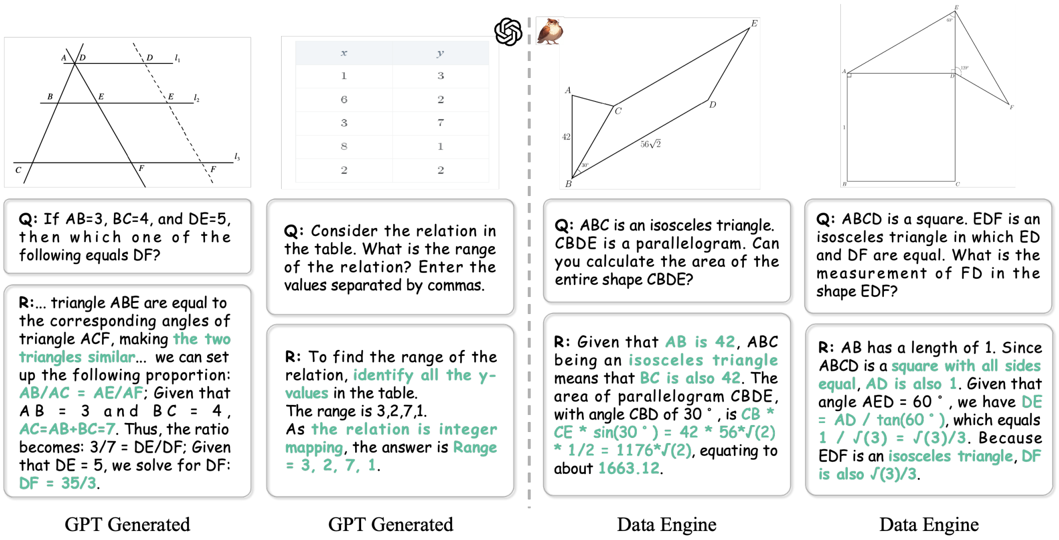

x	y
1	3
6	2
3	7
8	1
2	2

Q: If AB=3, BC=4, and DE=5, then which one of the following equals DF?

R:... triangle ABE are equal to the corresponding angles of triangle ACF, making the two triangles similar... we can set up the following proportion: AB/AC = AE/AF; Given that AB = 3 and BC = 4, AC=AB+BC=7. Thus, the ratio becomes: 3/7 = DE/DF; Given that DE = 5, we solve for DF: DF = 35/3.

GPT Generated

Q: Consider the relation in the table. What is the range of the relation? Enter the values separated by commas.

R: To find the range of the relation, identify all the y-values in the table.
The range is 3,2,7,1.
As the relation is integer mapping, the answer is Range = 3, 2, 7, 1.

GPT Generated

Q: ABC is an isosceles triangle. CBDE is a parallelogram. Can you calculate the area of the entire shape CBDE?

R: Given that AB is 42, ABC being an isosceles triangle means that BC is also 42. The area of parallelogram CBDE, with angle CBD of 30 ° , is CB * CE * sin(30 °) = 42 * 56*√(2) * 1/2 = 1176*√(2), equating to about 1663.12.

Data Engine

Q: ABCD is a square. EDF is an isosceles triangle in which ED and DF are equal. What is the measurement of FD in the shape EDF?

R: AB has a length of 1. Since ABCD is a square with all sides equal, AD is also 1. Given that angle AED = 60 ° , we have DE = AD / tan(60 °), which equals 1 / √(3) = √(3)/3. Because EDF is an isosceles triangle, DF is also √(3)/3.

Data Engine

Figure 10: **Accurate Rationale Examples in MAVIS-Instruct.** Most GPT-generated and Data Engine-generated rationales ensure correctness.

Table 3: **Statistics of MAVIS-Caption.**

Statistic	**Number**
Total Captions	
- Total number	588K
- Average length (words)	62.85
- Average length (characters)	339.68
- Vocabulary size	418
Plane Geometry	
- Total number	299K (50.9%)
- Average length (words)	69.77
- Average length (characters)	385.85
- Vocabulary size	195
Analytic Geometry	
- Total number	77K (13.1%)
- Average length (words)	39.64
- Average length (characters)	210.10
- Vocabulary size	158
Function	
- Total number	212K (36.0%)
- Average length (words)	61.48
- Average length (characters)	321.46
- Vocabulary size	149

Table 4: **Subject Distribution of MAVIS-Instruct.**

Statistic	**Number**
Total questions	834K
- Multiple-choice questions	615K (62.4%)
- Free-form questions	218K (37.6%)
Data Engine Generated Problems	582K
- Geometry questions	466K (80.0%)
- Function questions	116K (20.0%)
Data Engine Captions Annotated by GPT-4	51K
- Geometry questions	30K (58.8%)
- Function questions	21K (41.2%)
Manual Collection Augmented by GPT-4	83K
- Geometry questions	72K (86.5%)
- Function questions	11K (13.5%)
Existing Datasets Augmented by GPT-4	118K
- Geometry questions	118K (100.0%)
- Function questions	0 (0%)
Number of unique images	611K (73.3%)
Number of unique questions	804K (96.5%)
Number of unique answers	675K (81.0%)
Average question length	44.60
Average answer length	62.82

A.3 Ablation Study

A.3.1 MAVIS-Caption

To validate the enhancement of Math-CLIP's **diagram perception capability**, we sampled 100 validation diagram-caption pairs and computed their cosine similarity using both CLIP and Math-CLIP. The results, as shown in Table 5, indicate that Math-CLIP encodes more discriminative diagram features. Additionally, the attention visualization in Figure 1(a) of the main paper further demonstrates that Math-CLIP captures mathematical visual elements within diagrams more effectively, highlighting the efficacy of MAVIS-Caption.

To validate the role of MAVIS-Caption in second-stage training, we present both quantitative and qualitative results for diagram captioning on the same 100 validation pairs in the first column of Table 6. The use of MAVIS-Caption significantly enhances the **diagram understanding capability**. This shows that MAVIS-Caption helps the LLM generate accurate captions from diagrams, improving its ability to comprehend each visual token from Math-CLIP and align visual elements with textual descriptions. We also evaluated MAVIS's performance on MathVerse without second-stage training, as shown in the second column of Table 6. Without MAVIS-Caption training, the CoT reasoning quality of MAVIS-7B is somewhat compromised. This suggests that training the model in diagram captioning improves its **mathematical expression capability**, enabling it to produce language expressions that align with mathematical concepts. This foundational skill supports the generation of subsequent CoT reasoning steps.

Table 5: **Diagram Perception Enhancement by Math-CLIP**, using MAVIS-Caption in the first stage. We calculate the average cosine similarity among 100 validation diagram-caption pairs.

Vision Encoder	Matched Pair ↑	Unmatched Pair ↓
CLIP	0.22	0.24
Math-CLIP	**0.83**	**0.17**

A.3.2 MAVIS-Instruct

Redundant Text When curating questions for MAVIS-Instruct, we minimize the redundant content within the question texts, which refers to the directly observable content in the diagram, e.g., the

Table 6: **Diagram Understanding Enhancement** and **Mathematical Expression Enhancement** in LLM using MAVIS-Caption in the second Stage. We compare the METEOR and CIDEr scores for diagram captioning on 100 validation samples, as well as the accuracy and CoT evaluation results on MathVerse, both with and without the MAVIS-Caption training.

Training Data	Diagram-Caption Pairs		MathVerse	
	METEOR	CIDEr	Acc (%)	CoT-E (%)
w MAVIS-Caption	23.7	161.3	28.4	35.2
w/o MAVIS-Caption	14.0	69.4	25.6	32.8

presence of shapes or intersection points of functions. Such information is repetitive to visual components, and may assist MLLMs in bypassing the process of diagram interpretation, thereby harming their related skills. By mostly avoiding redundant texts in MAVIS-Instruct, our data enforces MLLMs to learn stronger **diagram interpretation capabilities**. In Table 7, we add redundant texts (diagram captions) to the Data Engine Generated Problems for training, leading to expected performance drop.

CoT Rationales For each instance in MAVIS-Instruct, we incorporate detailed rationales for problem-solving, either generated by GPT-4 or our rule-based data engine. In Table 8, we remove all intermediate rationales of each problem in MAVIS-Instruct, and train the model to directly output the final answer. As shown, both the CoT evaluation and accuracy scores are degraded. This demonstrates the significance of our rationale annotations, which effectively improves the CoT **reasoning capabilities** of MLLMs.

Table 7: **Diagram Interpretation Enhancement for MLLM**, using MAVIS-Instruct in the third stage. We compare the results by adding redundant texts (diagram captions) to the Data Engine Generated Problems within MAVIS-Instruct.

MAVIS-Instruct	MathVerse	GeoQA	FunctionQA
w/o Redundant Texts	**28.4**	**68.3**	**50.0**
w Redundant Texts	26.5	66.5	48.4

Table 8: **Reasoning Capability Enhancement for MLLM**, using MAVIS-Instruct in the third stage.

Training Data	MathVerse	
	Acc	CoT-E
w Rationales	**28.4**	**35.2**
w/o Rationales	25.2	26.6

A.3.3 COMPARED TO GENERAL VISUAL INSTRUCTION DATA

Since Mammoth-2 is a highly capable LLM for mathematical tasks, one possible question is whether simply integrating a vision encoder into Mammoth-2 and training it with conventional visual instruction tuning data would suffice for effectively solving visual-based mathematical problems. To compare MAVIS data with other visual instruction tuning datasets and investigate the specific benefits of MAVIS data in Mammoth-2 (7B), we conduct an ablation study. We utilize the data from LLaVA-NeXT (558K for pre-training and 760K for fine-tuning) and compare it with our MAVIS data (558K MAVIS-Caption for pre-training and 834K MAVIS-Instruct for fine-tuning). Performance is evaluated using the accuracy metric on MathVerse, excluding the DPO training stage for fairness.

Table 9: Ablation study results for comparison between MAVIS Data and other visual instruction tuning data. The first row in the table represents the original LLaVA-NeXT-8B.

Visual Encoder	**LLM**	**Pre-training**	**Fine-tuning**	**MathVerse Acc (%)**
CLIP	LLaMA-3 (8B)	LLaVA data	LLaVA data	15.6
CLIP	Mammoth-2 (7B)	LLaVA data	LLaVA data	18.3
CLIP	Mammoth-2 (7B)	LLaVA data	**MAVIS-Instruct**	25.7
CLIP	Mammoth-2 (7B)	**MAVIS-Caption**	**MAVIS-Instruct**	26.4
Math-CLIP	Mammoth-2 (7B)	**MAVIS-Caption**	**MAVIS-Instruct**	27.5

Based on the results presented in Table 9, we make the following observations:

1. **Mammoth-2 vs. LLaMA-3:** Mammoth-2 achieves a +2.7 improvement in accuracy compared to LLaMA-3, highlighting its prior knowledge and inherent capability in mathematical problem solving.
2. **Impact of MAVIS-Instruct:** Fine-tuning with MAVIS-Instruct significantly enhances performance by +7.4, underscoring the substantial advantage of our dataset for mathematical reasoning tasks compared to general visual instruction datasets.
3. **MAVIS-Caption and Math-CLIP:** Using MAVIS-Caption for pre-training and employing the Math-CLIP encoder further boosts performance, leading to enhanced mathematical visual perception and reasoning capabilities. Overall, our MAVIS data contributes a +9.2 improvement in accuracy over Mammoth-2 trained with LLaVA data.

A.3.4 Performance Across Different Subjects

Although MAVIS-Instruct contains a substantial number of high-quality solid geometry problems that were manually curated, our data engine only generates plane geometry and function problems. Therefore, we aim to evaluate the performance of the MAVIS model across different mathematical domains, specifically plane geometry, functions, and solid geometry. We provide the detailed subject scores of MAVIS-7B on MathVerse, comparing the CoT evaluation score (note that the subject-level accuracy scores are not publicly released) with other models on the official leaderboard.

Table 10: Performance comparison across different models on Plane Geometry, Solid Geometry, and Functions of MathVerse evaluation tasks.

Model	**All (CoT-Eval)**	**Plane Geometry**	**Solid Geometry**	**Functions**
LLaVA-NeXT	17.2	15.9	19.6	23.1
ShareGPT4V	17.4	16.9	15.0	20.2
SPHINX-MoE	22.8	24.5	15.8	19.5
InternLM-XC2	25.9	26.2	20.1	23.7
MAVIS-7B	**35.2**	**37.1**	**28.9**	**31.0**

The results shown in Table 10 demonstrate that our model achieves leading performance across all three subjects. Notably, its proficiency in plane geometry and functions can be attributed to the training with our meticulously curated MAVIS dataset. Additionally, for solid geometry, which shares similarities with plane geometry in both visual appearance and reasoning process, we believe that our model effectively generalizes its learned knowledge and reasoning capabilities, leading to enhanced performance in this domain as well.

A.3.5 Synthetic Data vs Real Data

In MAVIS-Instruct, we integrate both synthetic problems generated by the data engine (633K, 76%) and real-world problems augmented with GPT (201K, 24%). The synthetic data is composed of both geometry and function problems, while the real-world data primarily focuses on geometry. We conduct an ablation study to assess the contributions of these data components, excluding the DPO training stage to ensure fairness.

Table 11: Ablation study of synthetic and real data contributions to MAVIS-7B's performance.

Synthetic Data	**Real-world Data**	**MathVerse Acc (%)**	**GeoQA**	**FunctionQA**	**MMMU-Math**
✓	–	22.6	44.2	37.1	34.6
–	✓	24.3	66.4	25.8	29.8
✓	✓	27.5	66.7	40.3	39.2

The results shown in Table 11 indicate that the two data sources exhibit complementary characteristics, both playing a crucial role in achieving the final performance. Specifically, synthetic data significantly enhances the results on FunctionQA and MMMU-Math, as these benchmarks include a substantial proportion of function-related problems. Conversely, real-world data has a greater impact on GeoQA, given its stronger alignment with the geometry-focused nature of this benchmark.

A.3.6 Data Scaling

A good instruction tuning dataset should exhibit the characteristic of data scaling: as the dataset size increases, the model trained on it should demonstrate progressively better performance. To verify that MAVIS-Instruct possesses this property, we conduct an ablation study on the 834K MAVIS-Instruct dataset by randomly sampling 25%, 50%, and 75% of the data for instruction tuning, excluding the DPO stage. We then evaluate the models using the accuracy metric on MathVerse. The results, as shown in Table 12, indicate that the performance of MAVIS-7B consistently improves as the data scale increases. This demonstrates the promising potential of our dataset to further enhance mathematical reasoning capabilities with larger-scale utilization.

Table 12: Performance of MAVIS-7B at different data proportions.

25%	**50%**	**75%**	**100%**
23.3	25.7	26.9	27.5

Table 13: Comparison of different training settings.

LLMs	**Caption CIDEr**	**MathVerse Acc (%)**
Frozen	79.6	26.2
Unfrozen	146.2	28.1
LoRA-based	161.3	28.4

A.3.7 Generalization Ability

Although our Data Engine considers as many problem types as possible, it is inherently challenging for a manually designed engine to cover all possible types of mathematical visual diagrams. To alleviate this, we incorporate real-world data by manual collection and GPT augmentation, which well enhances the generalization capablitity of MAVIS-7B. In Figure 11, we selected examples involving inscribed triangles (they cannot be generated via our data engine) from publicly available math benchmarks, and tested MAVIS-7B on these examples, where our model performs accurate reasoning.

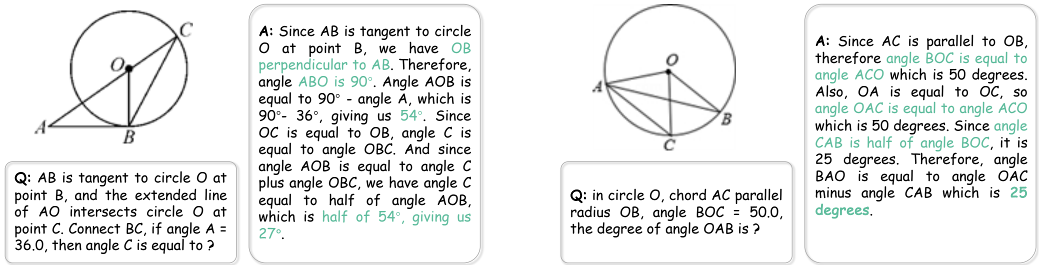

Q: AB is tangent to circle O at point B, and the extended line of AO intersects circle O at point C. Connect BC, if angle A = 36.0, then angle C is equal to ?

A: Since AB is tangent to circle O at point B, we have OB perpendicular to AB. Therefore, angle ABO is 90°. Angle AOB is equal to 90° - angle A, which is 90°- 36°, giving us 54°. Since OC is equal to OB, angle C is equal to angle OBC. And since angle AOB is equal to angle C plus angle OBC, we have angle C equal to half of angle AOB, which is half of 54°, giving us 27°.

Q: in circle O, chord AC parallel radius OB, angle BOC = 50.0, the degree of angle OAB is ?

A: Since AC is parallel to OB, therefore angle BOC is equal to angle ACO which is 50 degrees. Also, OA is equal to OC, so angle OAC is equal to angle ACO which is 50 degrees. Since angle CAB is half of angle BOC, it is 25 degrees. Therefore, angle BAO is equal to angle OAC minus angle CAB which is 25 degrees.

Figure 11: Examples for MAVIS-7B solving math problems with circumcircles of triangles.

A.3.8 Enhancing Vision-only Performance

To evaluate the impact of OCR datasets on MAVIS-7B's performance, we conducted an ablation study focusing on vision-only and vision-dominant problems in MathVerse. These problems require the model to interpret question texts rendered directly in diagrams, thus relying heavily on OCR capabilities. MAVIS-7B, however, was initially not trained with OCR-specific datasets, limiting its performance in these tasks.

In contrast, generalist models like LLaVA-NeXT include extensive OCR datasets such as OCRVQA, DocVQA, and SynDog-EN, which significantly enhance their OCR capabilities. To bridge this gap, we incorporated OCR datasets (OCRVQA and DocVQA) in our third-stage instruction tuning to improve MAVIS-7B's OCR performance.

The results, as shown in Table 14, indicate a notable improvement in vision-dominant and vision-only problems for MAVIS-7B after the inclusion of OCR datasets, highlighting the potential of better OCR integration for further boosting its performance. In Figure 12, we also showcase some failure cases of our MAVIS-7B with OCR training on vision-only problems. Although the vision-only results are improved via the OCR instruction dataset, the model still suffers from limited perception capabilities of questions and visual elements within the diagram. This indicates that the OCR capability is still the bottleneck of vision-only performance. We leave this as a future work to further enhance the OCR capabilities of MAVIS for mathematical visual elements.

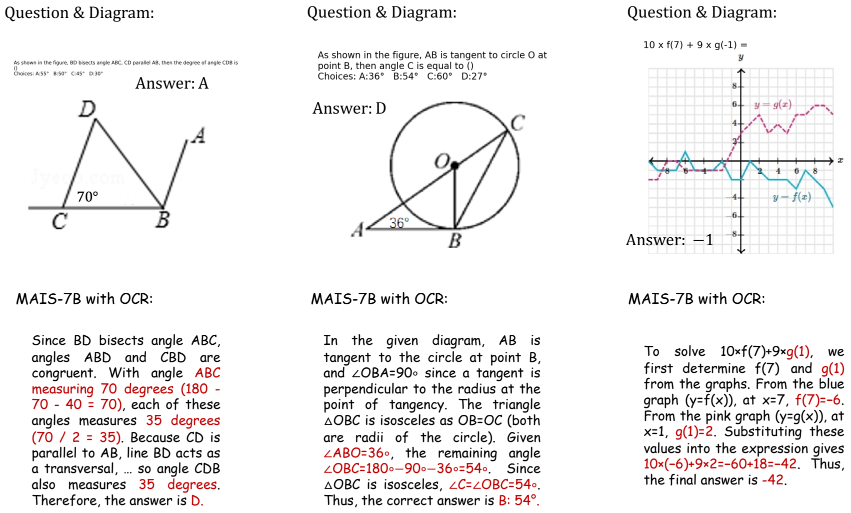

As shown in the figure, BD bisects angle ABC, CD parallel AB, then the degree of angle CDB is ()
Choices: A:55° B:50° C:45° D:30°

As shown in the figure, AB is tangent to circle O at point B, then angle C is equal to ()
Choices: A:36° B:54° C:60° D:27°

10 x f(7) + 9 x g(-1) =

Since BD bisects angle ABC, angles ABD and CBD are congruent. With angle ABC measuring 70 degrees (180 - 70 - 40 = 70), each of these angles measures 35 degrees (70 / 2 = 35). Because CD is parallel to AB, line BD acts as a transversal, … so angle CDB also measures 35 degrees. Therefore, the answer is D.

In the given diagram, AB is tangent to the circle at point B, and ∠OBA=90∘ since a tangent is perpendicular to the radius at the point of tangency. The triangle △OBC is isosceles as OB=OC (both are radii of the circle). Given ∠ABO=36∘, the remaining angle ∠OBC=180∘−90∘−36∘=54∘. Since △OBC is isosceles, ∠C=∠OBC=54∘. Thus, the correct answer is B: 54°.

To solve 10×f(7)+9×g(1), we first determine f(7) and g(1) from the graphs. From the blue graph (y=f(x)), at x=7, f(7)=-6. From the pink graph (y=g(x)), at x=1, g(1)=2. Substituting these values into the expression gives 10×(-6)+9×2=-60+18=-42. Thus, the final answer is -42.

Figure 12: Failure cases of MAVIS-7B with OCR training on vision-only problems.

Table 14: Impact of OCR data on solving vision-only problems.

Model	LLM Size	All	Text Dominant	Text Lite	Vision Intensive	Vision Dominant	Vision Only
LLaVA-NeXT	8B	15.6	19.4	15.2	16.8	15.2	11.3
LLaVA-NeXT	110B	24.5	31.7	24.1	21.0	22.1	20.7
MAVIS-7B	7B	28.4	**41.6**	**29.5**	**27.9**	24.7	18.3
MAVIS-7B w/ OCR	7B	**28.9**	40.8	29.2	27.4	**26.2**	**21.1**

A.3.9 Base LLM

We investigate different LLMs for the MAVIS model. As shown in Table 15, MAVIS is not very sensitive to LLM choices, and still surpasses previous models with the same LLM.

Table 15: **Performance Comparison using Different LLMs.** We compare the accuracy and CoT evaluation results on MathVerse.

Method	Base LLM	MathVerse	
		Acc	CoT-E
SPHINX-Plus	LLaMA2-13B	12.2	14.0
ShareGPT4V	Vicuna-13B	13.1	17.4
InternLM-XC2.	InternLM2-7B	16.5	25.9
MAVIS	LLaMA2-13B	24.5	30.7
	Vicuna-13B	24.8	30.6
	InternLM2-7B	28.0	33.8
	MAmmoTH2	**28.4**	**35.2**

A.3.10 Different Training Settings

Our training strategy is similar to LLaVA, but with key differences in the pre-training stage: we train both the projection layer and the LoRA-based LLM, whereas LLaVA only trains the projection layer. This design choice stems from the fundamental differences between general visual tasks and mathematical tasks:

1. For general visual tasks (e.g., LLaVA), training MLLMs typically requires the LLM to generate daily natural language responses, such as descriptive captions or instruction-following outputs. These outputs often rely on pre-existing knowledge within the pre-trained LLM. As a result, in LLaVA, there is no need to unfreeze the LLM to learn new types of outputs.
2. In contrast, for mathematical domains, LLMs need to generate math-specific responses, such as geometric descriptions, functional explanations, formulas, and theorems. These outputs often involve domain-specific knowledge not inherent in pre-trained LLMs. Given this, we incorporate learnable LoRA layers to infuse new knowledge into the LLM, enhancing its capability to produce high-quality mathematical expressions. Concurrently, we aim to prevent the LLM from overfitting to diagram captioning tasks during alignment. Therefore, using LoRA-based tuning allows us to preserve the LLM's generalizable pre-trained language knowledge while injecting specialized math-specific capabilities.

To further investigate the impact of different training settings on model performance, we conduct an ablation study comparing various LLM training settings during the alignment stage. We evaluate two tasks: the CIDEr score for diagram captioning on 100 validation samples (following the same setting as in Table 6 of the Appendix) and the accuracy score on MathVerse. The results, as shown in Table 13, indicate that the LoRA-based approach performs best, enabling MLLMs to generate high-quality mathematical captions while preserving pre-trained knowledge for improved problem-solving capabilities.

A.3.11 Enhancing a Pre-trained MLLM

To investigate whether our curated data and training techniques can improve the mathematical performance of a pre-trained large model (LLaVA-NeXT), we conducted an ablation study. Specifically, we progressively employed MAVIS-Instruct for instruction tuning, followed by DPO alignment on top of LLaVA-NeXT-8B, with both training stages performed for one epoch using a learning rate of 1×10^{-5}. The results, as shown in Table 16, demonstrate that these two continual training stages significantly enhance LLaVA-NeXT's ability to solve mathematical problems, with notable improvements across all evaluation categories.

Table 16: Performance improvement of LLaVA-NeXT-8B with MAVIS-Instruct and DPO alignment.

Model	LLM Size	All	Text Dominant	Text Lite	Vision Intensive	Vision Dominant	Vision Only
LLaVA-NeXT	8B	15.6	19.4	15.2	16.8	15.2	11.3
+ MAVIS-Instruct	8B	22.8	32.3	25.3	24.6	18.3	14.2
+ DPO	8B	**24.0**	**33.7**	**26.9**	**25.4**	**19.1**	**15.1**

A.4 Details of Automatic Data Engine

A.4.1 Diagram Generation

In this section, we detail the implementation specifics of the process for generating diagrams related to plane geometry, analytic geometry, and function domains.

Plane Geometry Diagram. Inspired by previous multi-hop reasoning methods (Kazemi et al., 2023; Wei et al., 2022; Nye et al., 2021), we employ an iterative generation method over logical theories to generate plane geometric images along with corresponding captions and question-answering pairs, whose complexity can be controlled across multiple axes. Specifically, we first define a set of fundamental geometric shapes in Figure 13.

Within each shape, new basic shapes can be generated by extending a particular edge. For each basic shape, we initially define a meta reasoning process:

$$O_{n-1}, C^i_{m_{n-1}} \xrightarrow{\mathrm{E}^i_{m_{n-1}}} O_n, i \in [1, z], \tag{1}$$

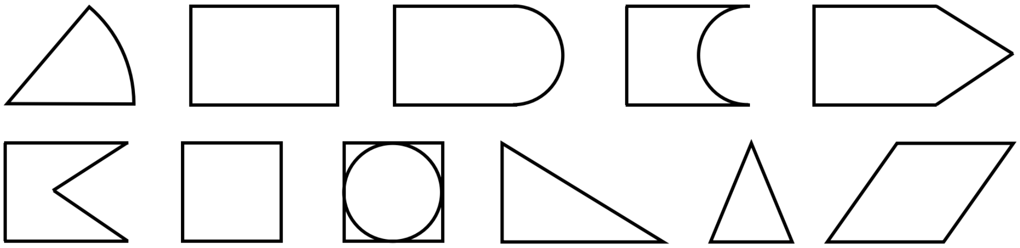

Figure 13: The set of fundamental shapes in plane geometry diagrams, whose straight edges can be extended into other basic shapes.

where O represents the initial side length of the shape, C_m denotes the additional conditions required to complete meta reasoning, and E_m provides a detailed explanation of the meta reasoning process. For example, when considering an isosceles triangle as the $(n-1)^{th}$ shape in a sequence, the vertex angle is still required as C_m to reason about base side length, and then to expand to the n^{th} shape, with E_m serving as the explanation of this process. The variable z indicates that there are z sets of possible meta reasoning for the shape, n indicates the length of the generating sequence, which is also the number of hops of reasoning required to answer the question. The initial side, extend side, and additional conditions for meta-reasoning of each basic shape can be referred to in Figure 13. In the final shape, question-answering pairs pertinent to this shape can be generated as

$$O_n, C^j_{q_n}, Q^j_n \xrightarrow{\mathrm{E}^j_{q_n}} A^j_n, j \in [1, m], \tag{2}$$

where C_q represents the additional conditions required to solve the problem, while Q and A denote the question and answer, respectively. E_q refers to the detailed explanation of the solving process. The variable m indicates that there are m pairs of question-answering and corresponding detailed explanations within the shape. By applying meta reasoning to the $n-1$th shape, the initial side length of the nth shape can be deduced. Therefore, for a complex composite figure consisting of n shapes, the overall question-answering pair can be defined as follows:

$$O_1, \sum_{k=1}^{n-1} C_{m_k}, C^j_{q_n}, Q^j_n \xrightarrow{\mathrm{E}^j_{q_n}} A^j_n. \tag{3}$$

Each shape defines a sufficient number of conditions, explanations, and answers to ensure the diversity of the generated question-answering pairs. Based on the aforementioned rules, controlling the length of the generation sequence can regulate the number of reasoning steps, and controlling the type of questions can manage the knowledge required for solving the problems. Thus, we can generate questions of varying difficulty levels, which can also be illustrated in Figure 14a.

Analytic Geometry Diagram. The image generation method for analytic geometry is relatively straightforward. First, we randomly select a range within the coordinate system: the minimum value of x is chosen as an integer between $[-12, -8]$, and the maximum value of x is chosen as an integer between $[8, 12]$; the range for y is the same as for x. Then, we define the following basic shapes: point, line segment, line, circle, ellipse, rectangle, square, polygon, and sector. During the generation process, we select a number between 1 and 4 as the number of shapes to generate. The generation rule is that **nonlinear shapes** other than points, line segments, and lines **must not overlap**.

Function Diagram. The generation of function graphs is also straightforward as shown in Figure 14b. We define the following basic functions, each with a set of parameters that can be randomly selected:

Sine Function $y = A \cdot \sin(f \cdot x + \phi)$, where the amplitude A is a random integer between 1 and 3, the frequency f is either 1 or 2, and the phase ϕ is a random integer between 0 and 2π.

Cosine Function $y = A \cdot \cos(f \cdot x + \phi)$, where the amplitude A is a random integer between 1 and 3, the frequency f is either 1 or 2, and the phase ϕ is a random integer between 0 and 2π.

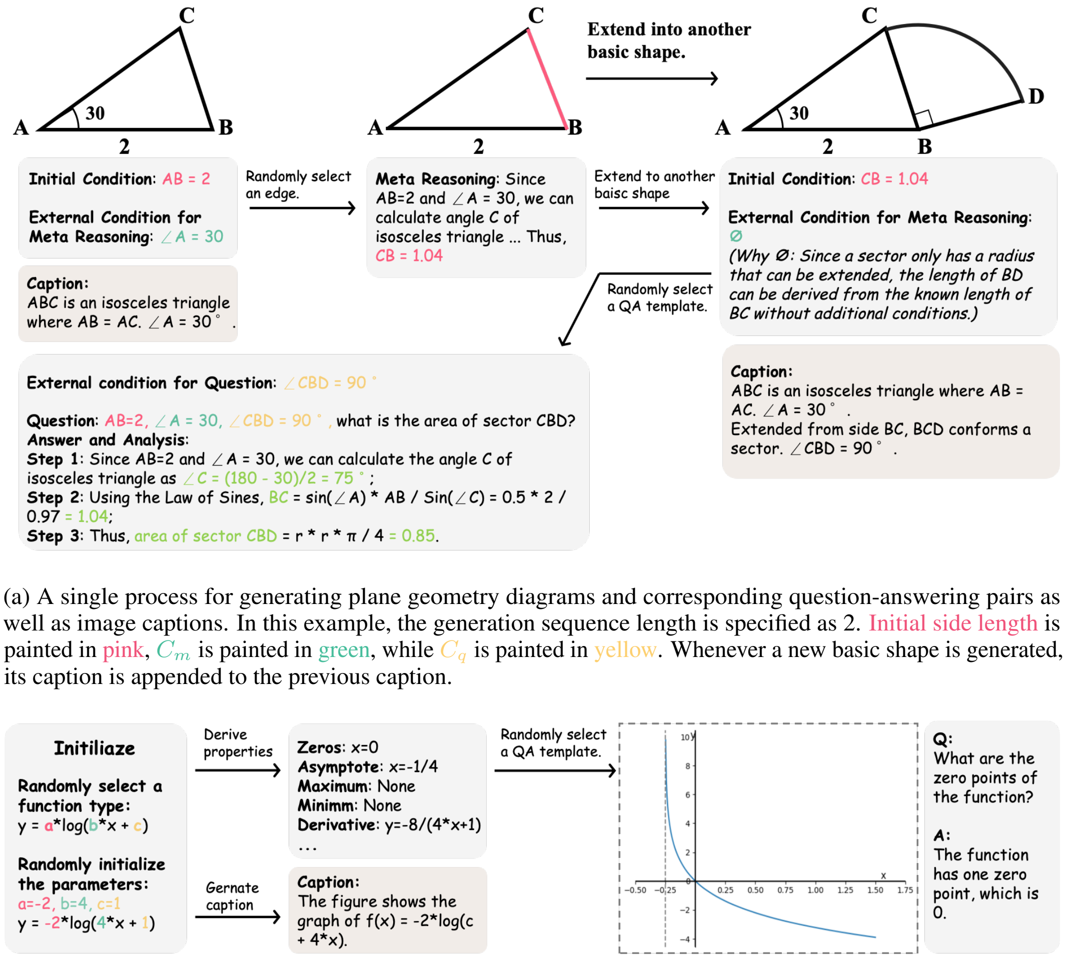
C
A
30
B
2
C
A
B
2
Extend into another basic shape.
C
D
A
30
2
B
Randomly select an edge.
Extend to another baisc shape
Randomly select a QA template.

Initial Condition: AB = 2

External Condition for Meta Reasoning: ∠A = 30

Caption:
ABC is an isosceles triangle where AB = AC. ∠A = 30° .

Meta Reasoning: Since AB=2 and ∠A = 30, we can calculate angle C of isosceles triangle ... Thus, CB = 1.04

Initial Condition: CB = 1.04

External Condition for Meta Reasoning:
∅
(Why ∅: Since a sector only has a radius that can be extended, the length of BD can be derived from the known length of BC without additional conditions.)

Caption:
ABC is an isosceles triangle where AB = AC. ∠A = 30° .
Extended from side BC, BCD conforms a sector. ∠CBD = 90° .

External condition for Question: ∠CBD = 90°

Question: AB=2, ∠A = 30, ∠CBD = 90° , what is the area of sector CBD?
Answer and Analysis:
Step 1: Since AB=2 and ∠A = 30, we can calculate the angle C of isosceles triangle as ∠C = (180 - 30)/2 = 75° ;
Step 2: Using the Law of Sines, BC = sin(∠A) * AB / Sin(∠C) = 0.5 * 2 / 0.97 = 1.04;
Step 3: Thus, area of sector CBD = r * r * π / 4 = 0.85.

(a) A single process for generating plane geometry diagrams and corresponding question-answering pairs as well as image captions. In this example, the generation sequence length is specified as 2. Initial side length is painted in pink, C_m is painted in green, while C_q is painted in yellow. Whenever a new basic shape is generated, its caption is appended to the previous caption.

Initiliaze

Randomly select a function type:
y = a*log(b*x + c)

Randomly initialize the parameters:
a=-2, b=4, c=1
y = -2*log(4*x + 1)

Zeros: x=0
Asymptote: x=-1/4
Maximum: None
Minimm: None
Derivative: y=-8/(4*x+1)
...

Caption:
The figure shows the graph of f(x) = -2*log(c + 4*x).

Q:
What are the zero points of the function?

A:
The function has one zero point, which is 0.

(b) A single process is used for generating function diagrams along with the corresponding question-answer pairs and image captions. Once the functional expression is determined, all its properties can be directly computed, and the function plot can be generated accordingly. The caption for the function diagram simply states the functional expression.

Figure 14: The pipeline of our data engine, consisting of (a) the generation of plane geometry diagrams and (b) the generation of function diagrams.

Tangent Function $y = A \cdot \tan(f \cdot x + \phi)$, where the amplitude A is a random integer between 1 and 3, the frequency f is either 1 or 2, and the phase ϕ is a random integer between 0 and 2π.

Polynomial Function $P(x) = a_n x^n + a_{n-1} x^{n-1} + \cdots + a_1 x + a_0$, where the degree n is a random integer between 1 and 4. The coefficients a_i are randomly selected integers ranging from -3 to 3.

piece-wise Function piece-wise polynomial functions are divided into 2 or 3 segments, with each segment's parameters identical to those of a polynomial function.

Logarithmic Function $y = a \cdot \log_b(c \cdot x + d)$, where the coefficient a is randomly chosen from $\{-3, -2, -1, 1, 2, 3\}$, the base b is randomly chosen from $\{2, 10, \lfloor e \rfloor\}$, the coefficient c is a random integer between 1 and 3, and the coefficient d is a random integer between 1 and 6, ensuring that $c \cdot x + d$ is positive.

Absolute Function $y = |a \cdot x + b|$, where a and b are random integer between -5 and 5.

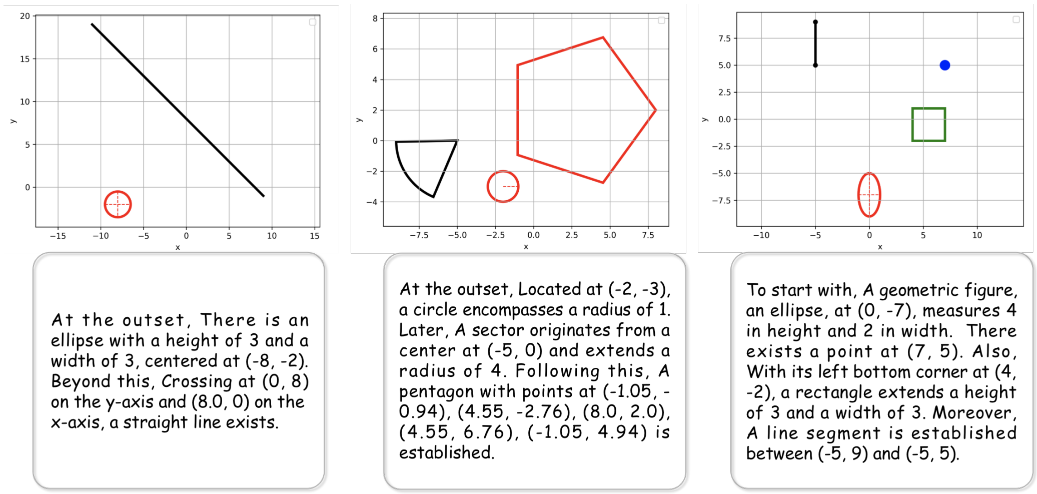

At the outset, There is an ellipse with a height of 3 and a width of 3, centered at (-8, -2). Beyond this, Crossing at (0, 8) on the y-axis and (8.0, 0) on the x-axis, a straight line exists.

At the outset, Located at (-2, -3), a circle encompasses a radius of 1. Later, A sector originates from a center at (-5, 0) and extends a radius of 4. Following this, A pentagon with points at (-1.05, -0.94), (4.55, -2.76), (8.0, 2.0), (4.55, 6.76), (-1.05, 4.94) is established.

To start with, A geometric figure, an ellipse, at (0, -7), measures 4 in height and 2 in width. There exists a point at (7, 5). Also, With its left bottom corner at (4, -2), a rectangle extends a height of 3 and a width of 3. Moreover, A line segment is established between (-5, 9) and (-5, 5).

Figure 15: Examples of analytical geometry diagram caption.

We first determine the domain range to be displayed on the function graph. For trigonometric functions, the domain is set to $[-\pi, \pi]$. For piece-wise polynomial functions, the minimum value of x is a random integer between $[-12, -8]$, and the maximum value of x is a random integer between $[8, 12]$. For other functions, the minimum and maximum values of x are random integers within the ranges of $[-6, -3]$ and $[3, 6]$, respectively. During the plotting process, we calculate the local maxima, minima, and zeros of the function by iterating through the domain. We then render the x-coordinates of these extrema and zeros on the x-axis of the function graph.

A.4.2 MAVIS-Caption

In this section, we detail how the captions corresponding to images in the MAVIS-Caption Dataset are generated with our automatic data engine.

Plane Geometry Caption. Based on the generation process described in Section A.4.1, when generating each shape, a caption is randomly selected from a set of captions for that shape and some connecting words are randomly added. We also randomly select some edges or angles and state their measurements in the caption. After generating the raw caption, we use GPT-3.5 to refine it, enhancing its linguistic structure and semantic diversity. An example is shown in Figure **??**.

Function Caption. According to the function graph generation process described in Section A.4.1, we record the function's zeros and extrema. Additionally, we also record the function's expression and asymptotes. These attributes are incorporated into a randomly selected caption template to form the function graph's caption. Some examples are provided in Figure 16.

Analytic Geometry Caption. For each shape, we maintain a set of caption templates that describe the shape's type, coordinate position, and other attributes. In the generation process described in Section A.4.1, we select a template and randomly add some diverse connecting words to form a complete caption. Examples of some captions are shown in Figure 15.

A.4.3 MAVIS-Instruct

Manual Collection Augmented by GPT-4. To complement the dataset with real-world problem-solving scenarios, we hire 8 human experts to manually collect visual math problems from various public sources[1,2,3], spanning plane geometry, analytic geometry, and function. For problems, we try to obtain their content as complete as possible, including questions, diagrams, answers, and rationales if available. The collection process consists of the following steps:

1. **Problem Collection:** We gathered problems from three public sources as comprehensively as possible, including questions, diagrams, answers, category information, and rationales where

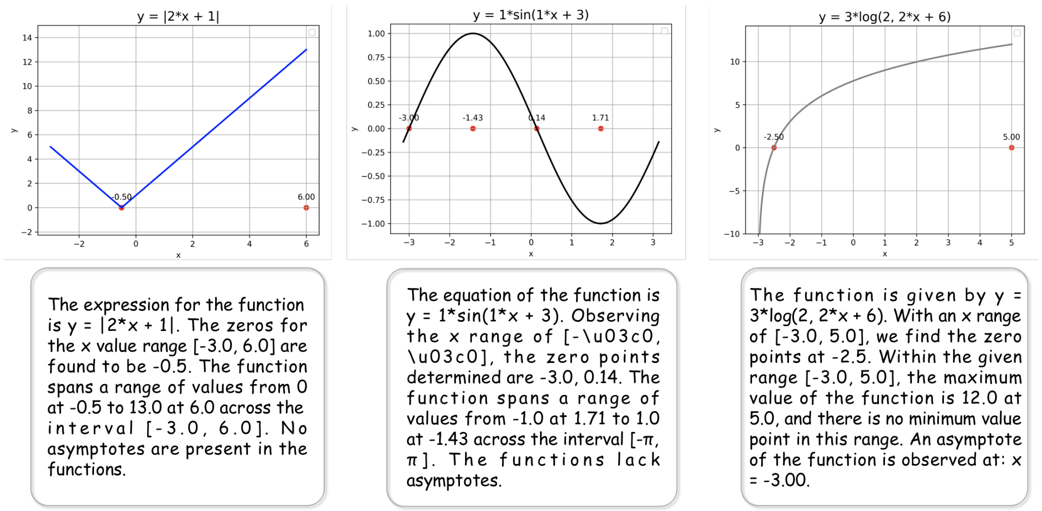

The expression for the function is y = |2*x + 1|. The zeros for the x value range [-3.0, 6.0] are found to be -0.5. The function spans a range of values from 0 at -0.5 to 13.0 at 6.0 across the interval [-3.0, 6.0]. No asymptotes are present in the functions.

The equation of the function is y = 1*sin(1*x + 3). Observing the x range of [-\u03c0, \u03c0], the zero points determined are -3.0, 0.14. The function spans a range of values from -1.0 at 1.71 to 1.0 at -1.43 across the interval [-π, π]. The functions lack asymptotes.

The function is given by y = 3*log(2, 2*x + 6). With an x range of [-3.0, 5.0], we find the zero points at -2.5. Within the given range [-3.0, 5.0], the maximum value of the function is 12.0 at 5.0, and there is no minimum value point in this range. An asymptote of the function is observed at: x = -3.00.

Figure 16: Function diagram captions.

available. The problems are primarily at the high-school level, covering plane geometry and functions (including analytic geometry).

2. **Data Verification:** Based on their initial categories (subject, subfield, and difficulty level), the problems were organized into distinct groups. Six expert annotators were tasked with meticulously verifying the correctness and completeness of each problem. They refined the detailed chain-of-thought (CoT) rationales and *ensured that there was no overlap with evaluation data by visually inspecting the diagrams*. This rigorous verification process resulted in a total of 4K verified problems.

3. **Text-lite Construction:** To optimize the problems for training mathematical visual capabilities, the 4K problems were processed using GPT-4V with a customized prompt (as shown in Figure 15). This step involved removing redundant information from the question text to create concise, text-lite problems, specifically tailored to our training objectives.

Then, we first feed all the related information into GPT-4V to eliminate the redundant information within text questions, constructing the text-lite version of problems by the prompt in Figure 17. Then, we design three types of prompts for GPT-4 to augment 15 multiple-choice questions (including 10 multiple-choice and 5 binary-choice, i.e., 'True' or 'False') and 5 free-form questions, respectively, as shown in Figure 18. We do not adopt GPT-4V here, since GPT-4V itself would misunderstand diagrams for low-quality data augmentation. The newly generated problems contain detailed CoT rationales and diverse question forms.

Existing Datasets Augmented by GPT-4. Previous efforts have been made to provide some small-scale, plane geometry datasets, e.g., GeoQA (Chen et al., 2021c), GeoQA+ (Chen et al., 2021a), and Geometry3K (Lu et al., 2021). Although they are limited in data scale for tuning MLLMs and include no rationales, we can also regard them as a seed dataset and adopt GPT-4 to augment larger-scale training data. We do not utilize GPT-4V here for the same reason aforementioned. In detail, we design 3 types of question generation approaches using different prompts, as shown in Figure 19. For Geometry3K, as the question texts are normally brief and contain marginal descriptive information, posing challenges for GPT-4 to understand the diagram, we only augment them to generate binary-choice questions, i.e., 'Ture' or 'False'. For GeoQA+, we can leverage the sufficient redundant information within their texts to generate more diverse and accurate multi-choice and free-form questions. Likewise, GPT-4 can produce CoT rationales for each problem.

[1] https://homework.study.com

[2] https://www.ixl.com/math

[3] https://mathspace.co/us

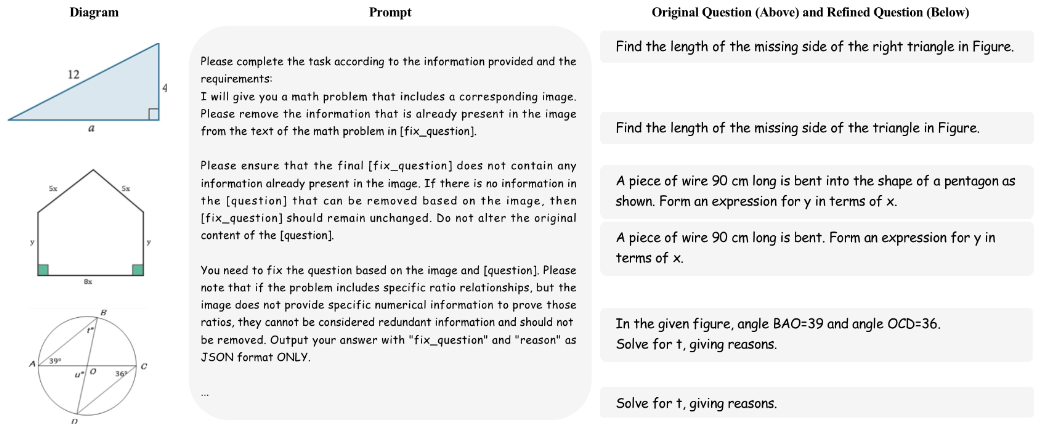

Diagram

Prompt

Please complete the task according to the information provided and the requirements:
I will give you a math problem that includes a corresponding image. Please remove the information that is already present in the image from the text of the math problem in [fix_question].

Please ensure that the final [fix_question] does not contain any information already present in the image. If there is no information in the [question] that can be removed based on the image, then [fix_question] should remain unchanged. Do not alter the original content of the [question].

You need to fix the question based on the image and [question]. Please note that if the problem includes specific ratio relationships, but the image does not provide specific numerical information to prove those ratios, they cannot be considered redundant information and should not be removed. Output your answer with "fix_question" and "reason" as JSON format ONLY.

...

Original Question (Above) and Refined Question (Below)

Find the length of the missing side of the right triangle in Figure.

Find the length of the missing side of the triangle in Figure.

A piece of wire 90 cm long is bent into the shape of a pentagon as shown. Form an expression for y in terms of x.

A piece of wire 90 cm long is bent. Form an expression for y in terms of x.

In the given figure, angle BAO=39 and angle OCD=36.
Solve for t, giving reasons.

Solve for t, giving reasons.

Figure 17: Manually collect visual math problems text-lite version.

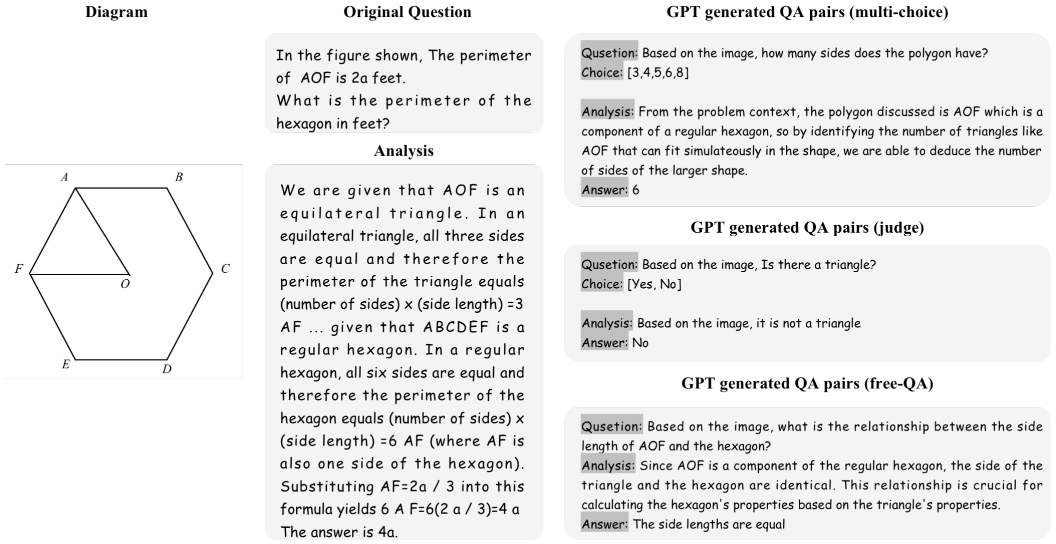

Diagram

Original Question

In the figure shown, The perimeter of AOF is 2a feet.
What is the perimeter of the hexagon in feet?

Analysis

We are given that AOF is an equilateral triangle. In an equilateral triangle, all three sides are equal and therefore the perimeter of the triangle equals (number of sides) x (side length) =3 AF ... given that ABCDEF is a regular hexagon. In a regular hexagon, all six sides are equal and therefore the perimeter of the hexagon equals (number of sides) x (side length) =6 AF (where AF is also one side of the hexagon). Substituting AF=2a / 3 into this formula yields 6 A F=6(2 a / 3)=4 a
The answer is 4a.

GPT generated QA pairs (multi-choice)

Qusetion: Based on the image, how many sides does the polygon have?
Choice: [3,4,5,6,8]

Analysis: From the problem context, the polygon discussed is AOF which is a component of a regular hexagon, so by identifying the number of triangles like AOF that can fit simulateously in the shape, we are able to deduce the number of sides of the larger shape.
Answer: 6

GPT generated QA pairs (judge)

Qusetion: Based on the image, Is there a triangle?
Choice: [Yes, No]

Analysis: Based on the image, it is not a triangle
Answer: No

GPT generated QA pairs (free-QA)

Qusetion: Based on the image, what is the relationship between the side length of AOF and the hexagon?
Analysis: Since AOF is a component of the regular hexagon, the side of the triangle and the hexagon are identical. This relationship is crucial for calculating the hexagon's properties based on the triangle's properties.
Answer: The side lengths are equal

Figure 18: We design different types of prompts for GPT-4 to augment 15 multiple-choice questions and 5 free-form questions, respectively.

Data Engine Captions Annotated by GPT-4. Given the delicately designed data engine for automatic diagram-caption creation, we can utilize the generated large-scale pairs to annotate question-answering data using GPT-4V. Different from the previous two sources that augment questions based on questions, we utilize the GPT-4V model here for caution data with two reasons: first, the detailed caption from our data engine can well guide GPT-4V for relatively higher-quality visual embedding; second, the visual input serves as guidance to provide additional spatial information for broad question forms. As shown in Figure 27 and Figure 28, we adopt different prompts for function and plane geometry problems, ensuring that the generated question-answering data is of high quality for instruction tuning.

Data Engine Generated Problems:

PLANE GEOMETRY. Based on the generation process described in Section A.4.1, we pose questions about the final shape in the generation sequence. We designed 6 types of questions: finding the perimeter, finding the area, finding the base length, finding the angle, finding the arc length, and finding the extended edge length. Each type of question has a set of templates that can be randomly

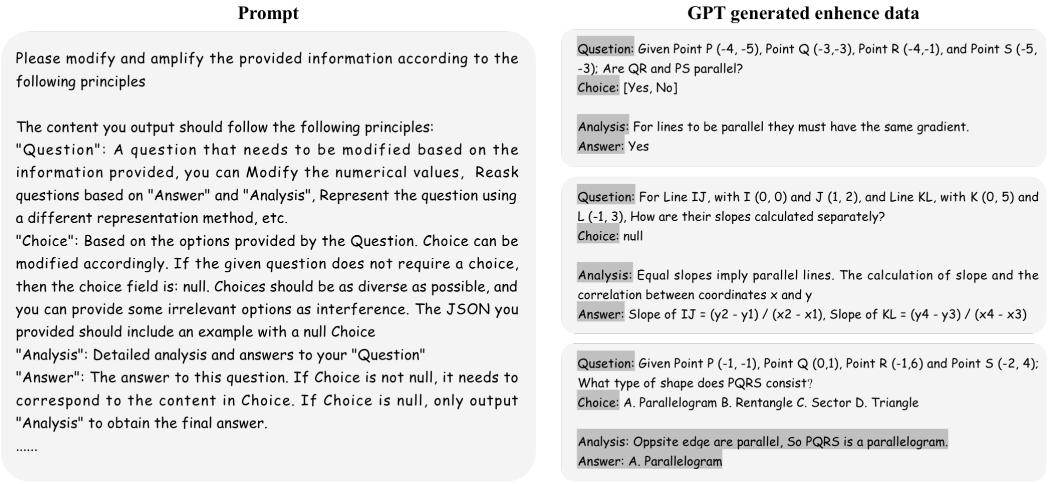

Prompt

Please modify and amplify the provided information according to the following principles

The content you output should follow the following principles:
"Question": A question that needs to be modified based on the information provided, you can Modify the numerical values, Reask questions based on "Answer" and "Analysis", Represent the question using a different representation method, etc.
"Choice": Based on the options provided by the Question. Choice can be modified accordingly. If the given question does not require a choice, then the choice field is: null. Choices should be as diverse as possible, and you can provide some irrelevant options as interference. The JSON you provided should include an example with a null Choice
"Analysis": Detailed analysis and answers to your "Question"
"Answer": The answer to this question. If Choice is not null, it needs to correspond to the content in Choice. If Choice is null, only output "Analysis" to obtain the final answer.
......

GPT generated enhence data

Qusetion: Given Point P (-4, -5), Point Q (-3,-3), Point R (-4,-1), and Point S (-5, -3); Are QR and PS parallel?
Choice: [Yes, No]

Analysis: For lines to be parallel they must have the same gradient.
Answer: Yes

Qusetion: For Line IJ, with I (0, 0) and J (1, 2), and Line KL, with K (0, 5) and L (-1, 3), How are their slopes calculated separately?
Choice: null

Analysis: Equal slopes imply parallel lines. The calculation of slope and the correlation between coordinates x and y
Answer: Slope of IJ = (y2 - y1) / (x2 - x1), Slope of KL = (y4 - y3) / (x4 - x3)

Qusetion: Given Point P (-1, -1), Point Q (0,1), Point R (-1,6) and Point S (-2, 4); What type of shape does PQRS consist?
Choice: A. Parallelogram B. Rentangle C. Sector D. Triangle

Analysis: Oppsite edge are parallel, So PQRS is a parallelogram.
Answer: A. Parallelogram

Figure 19: We design 3 types of question generation approaches using different prompts to augment existing visual mathematical dataset.

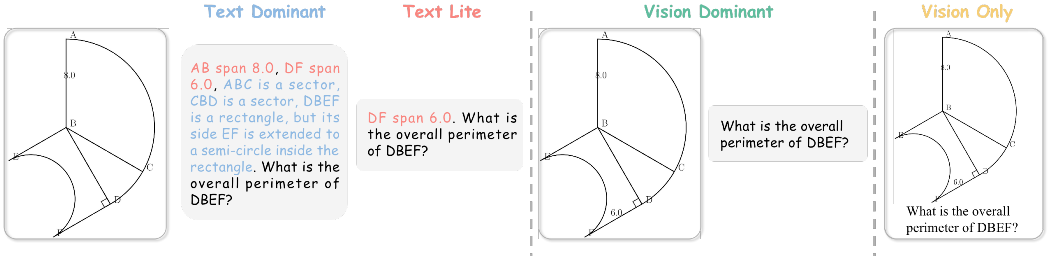

AB span 8.0, DF span 6.0, ABC is a sector, CBD is a sector, DBEF is a rectangle, but its side EF is extended to a semi-circle inside the rectangle. What is the overall perimeter of DBEF?

DF span 6.0. What is the overall perimeter of DBEF?

What is the overall perimeter of DBEF?

What is the overall perimeter of DBEF?

Figure 20: The Text Dominant, Text Lite, Vision Dominant, and Vision Only versions of the same question. Text Dominant and Text Lite use the same image. In the text, the necessary conditions for solving the problem are highlighted in red, while redundant descriptive conditions are highlighted in blue. In the Vision Only version, the question is rendered in the image, with no textual format.

selected, as shown in Figure 21-26. As for the answer and analysis, each shape has a set of templates for different types of questions to choose from, as shown in Section A.4.1.

To further enhance the model's understanding of different forms of questions and better utilize the diverse modal information in the text and images, we divided the plain geometry questions generated by the Data Engine into four versions referring to MathVerse (Zhang et al., 2024b): Text Dominant, Text Lite, Vision Dominant, and Vision Only.

Text Dominant We marked all the conditions required for solving the problem in the diagram and also described these conditions in the text, along with some redundant descriptive text.

Text Lite All the conditions required for solving the problem are randomly divided into two parts: one part is marked in the diagram, and the other part is described in the text. In other words, the conditions in the diagram and the conditions in the text do not overlap.

Vision Dominant All the conditions required for solving the problem are marked in the diagram, while the text only contains the question without any conditions.

Vision Only Not only are all the conditions required for solving the problem marked in the diagram, but the question is also rendered in the diagram, leaving the text portion empty.

The differences among the four versions of the same question are illustrated in Figure 20. Each basic shape will retain a set of redundant conditions. During the shape generation process, there is a 50% probability of including these redundant conditions.

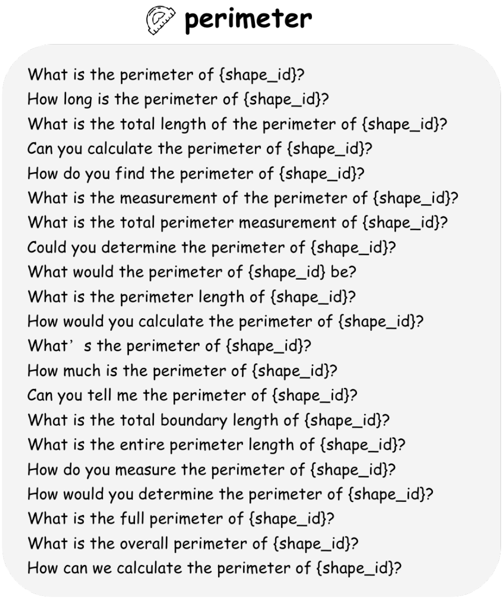

perimeter

What is the perimeter of {shape_id}?
How long is the perimeter of {shape_id}?
What is the total length of the perimeter of {shape_id}?
Can you calculate the perimeter of {shape_id}?
How do you find the perimeter of {shape_id}?
What is the measurement of the perimeter of {shape_id}?
What is the total perimeter measurement of {shape_id}?
Could you determine the perimeter of {shape_id}?
What would the perimeter of {shape_id} be?
What is the perimeter length of {shape_id}?
How would you calculate the perimeter of {shape_id}?
What’ s the perimeter of {shape_id}?
How much is the perimeter of {shape_id}?
Can you tell me the perimeter of {shape_id}?
What is the total boundary length of {shape_id}?
What is the entire perimeter length of {shape_id}?
How do you measure the perimeter of {shape_id}?
How would you determine the perimeter of {shape_id}?
What is the full perimeter of {shape_id}?
What is the overall perimeter of {shape_id}?
How can we calculate the perimeter of {shape_id}?

Figure 21: Perimeter problem templates.

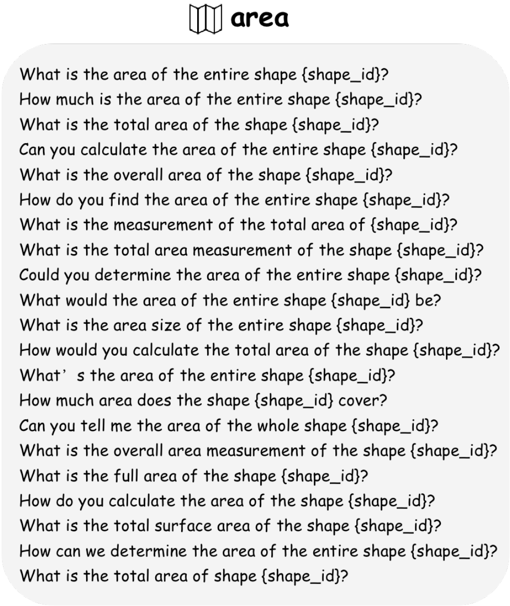

area

What is the area of the entire shape {shape_id}?
How much is the area of the entire shape {shape_id}?
What is the total area of the shape {shape_id}?
Can you calculate the area of the entire shape {shape_id}?
What is the overall area of the shape {shape_id}?
How do you find the area of the entire shape {shape_id}?
What is the measurement of the total area of {shape_id}?
What is the total area measurement of the shape {shape_id}?
Could you determine the area of the entire shape {shape_id}?
What would the area of the entire shape {shape_id} be?
What is the area size of the entire shape {shape_id}?
How would you calculate the total area of the shape {shape_id}?
What’ s the area of the entire shape {shape_id}?
How much area does the shape {shape_id} cover?
Can you tell me the area of the whole shape {shape_id}?
What is the overall area measurement of the shape {shape_id}?
What is the full area of the shape {shape_id}?
How do you calculate the area of the shape {shape_id}?
What is the total surface area of the shape {shape_id}?
How can we determine the area of the entire shape {shape_id}?
What is the total area of shape {shape_id}?

Figure 22: Area problem templates.

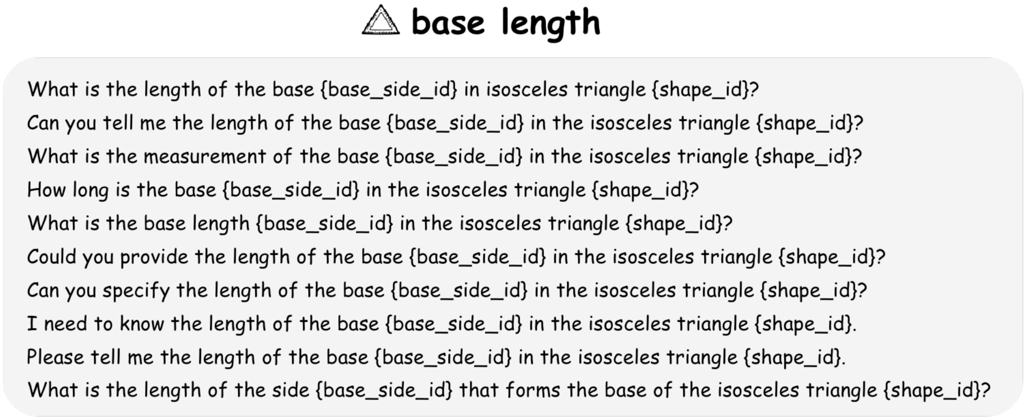

base length

What is the length of the base {base_side_id} in isosceles triangle {shape_id}?
Can you tell me the length of the base {base_side_id} in the isosceles triangle {shape_id}?
What is the measurement of the base {base_side_id} in the isosceles triangle {shape_id}?
How long is the base {base_side_id} in the isosceles triangle {shape_id}?
What is the base length {base_side_id} in the isosceles triangle {shape_id}?
Could you provide the length of the base {base_side_id} in the isosceles triangle {shape_id}?
Can you specify the length of the base {base_side_id} in the isosceles triangle {shape_id}?
I need to know the length of the base {base_side_id} in the isosceles triangle {shape_id}.
Please tell me the length of the base {base_side_id} in the isosceles triangle {shape_id}.
What is the length of the side {base_side_id} that forms the base of the isosceles triangle {shape_id}?

Figure 23: Base length problem templates.

FUNCTION. All functions will be examined with two types of questions: finding the derivative and finding the extrema. After obtaining the derivative, we calculate whether the derivative has zeros within the given domain. The presence of zeros determines the method for calculating the extrema.

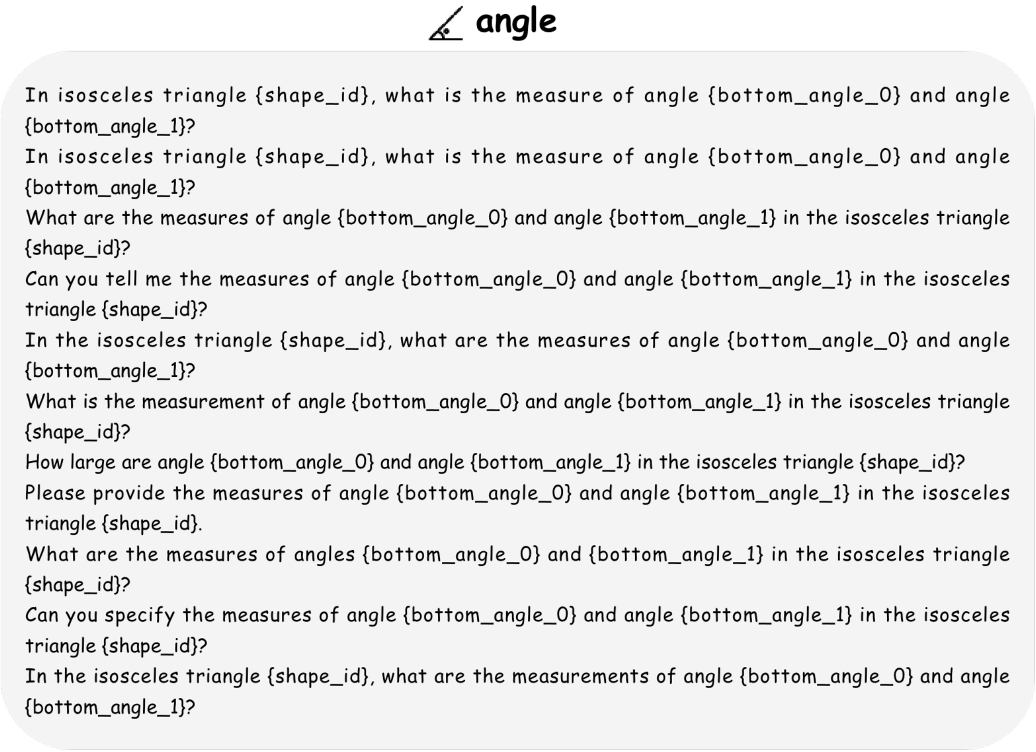

angle

In isosceles triangle {shape_id}, what is the measure of angle {bottom_angle_0} and angle {bottom_angle_1}?
In isosceles triangle {shape_id}, what is the measure of angle {bottom_angle_0} and angle {bottom_angle_1}?
What are the measures of angle {bottom_angle_0} and angle {bottom_angle_1} in the isosceles triangle {shape_id}?
Can you tell me the measures of angle {bottom_angle_0} and angle {bottom_angle_1} in the isosceles triangle {shape_id}?
In the isosceles triangle {shape_id}, what are the measures of angle {bottom_angle_0} and angle {bottom_angle_1}?
What is the measurement of angle {bottom_angle_0} and angle {bottom_angle_1} in the isosceles triangle {shape_id}?
How large are angle {bottom_angle_0} and angle {bottom_angle_1} in the isosceles triangle {shape_id}?
Please provide the measures of angle {bottom_angle_0} and angle {bottom_angle_1} in the isosceles triangle {shape_id}.
What are the measures of angles {bottom_angle_0} and {bottom_angle_1} in the isosceles triangle {shape_id}?
Can you specify the measures of angle {bottom_angle_0} and angle {bottom_angle_1} in the isosceles triangle {shape_id}?
In the isosceles triangle {shape_id}, what are the measurements of angle {bottom_angle_0} and angle {bottom_angle_1}?

Figure 24: Angle problem templates.

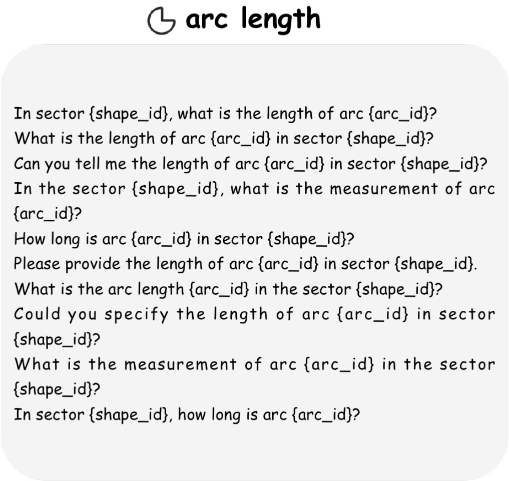

arc length

In sector {shape_id}, what is the length of arc {arc_id}?
What is the length of arc {arc_id} in sector {shape_id}?
Can you tell me the length of arc {arc_id} in sector {shape_id}?
In the sector {shape_id}, what is the measurement of arc {arc_id}?
How long is arc {arc_id} in sector {shape_id}?
Please provide the length of arc {arc_id} in sector {shape_id}.
What is the arc length {arc_id} in the sector {shape_id}?
Could you specify the length of arc {arc_id} in sector {shape_id}?
What is the measurement of arc {arc_id} in the sector {shape_id}?
In sector {shape_id}, how long is arc {arc_id}?

Figure 25: Arc length problem templates.

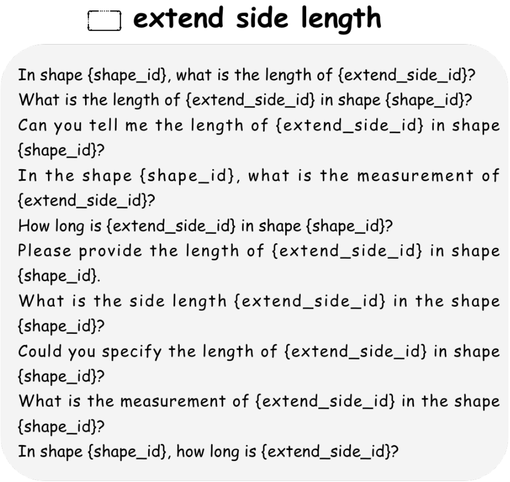

extend side length

In shape {shape_id}, what is the length of {extend_side_id}?
What is the length of {extend_side_id} in shape {shape_id}?
Can you tell me the length of {extend_side_id} in shape {shape_id}?
In the shape {shape_id}, what is the measurement of {extend_side_id}?
How long is {extend_side_id} in shape {shape_id}?
Please provide the length of {extend_side_id} in shape {shape_id}.
What is the side length {extend_side_id} in the shape {shape_id}?
Could you specify the length of {extend_side_id} in shape {shape_id}?
What is the measurement of {extend_side_id} in the shape {shape_id}?
In shape {shape_id}, how long is {extend_side_id}?

Figure 26: Extend side length problem templates.

Diagram:

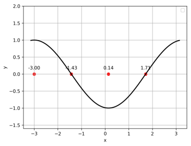

Caption:

The function can be described by the equation y = 1*cos(1*x + 3). With an x range of [-**π**, **π**], we find the zero points at -1.43, 1.71. Exploring the function within the range [-**π**, **π**], we find that the highest value it reaches is 1.0 at -3.0, and the lowest value is -1.0 at 0.14. There are no asymptotes in the functions.

Prompt for Function Problems:

Here is some more supplementary information for the diagram I give you: "{caption}"
Please first watch the diagram and ask a question that can be correctly answered only by seeing the diagram.
Then you should correctly analysis the question and give the answer.
The reasoning process should not use "According to the caption" or something like that.
Next, you should give 3 other hard false choices along with the correct one.

You should totally provide 3 questions.
The type of questions is multi-choice.

You should strictly follow this format and order (end every problem with ####):
QUESTION: What is the maximum value of the function in the given range?
ANALYSIS: From the diagram, we can observe that when x=0, the function obtain the maximum value, which is 4.
ANSWER: B. 4
CHOICE: A. 3; B. 4; C. 2; D. 1 ####

Question & Rationale Generated by GPT-4V:

Question:
What is the length of square side FG? Choices: A. 10.0; B. 10.1; C. 9.9; D. 10.5

Rational:
Since FG is a side of square DBFG, and the properties of a square dictate that all sides are equal in length, the length of FG must be the same as DB which is given as 10.0 units. So the answer is A.

Question:
What is the length of diagonal AC in triangle ABC? Choices: A. 10.1; B. 9.8; C. 9.9; D. 10.0

Rational:
In right triangle ABC with sides AB = 7.0 and BC = 7.0 units, and angle ACB = 45°, the triangle is isosceles. The length of diagonal AC can be calculated using the Pythagorean theorem: $AC = \sqrt{}(AB^2 + BC^2) = \sqrt{}(7.0^2 + 7.0^2) = \sqrt{98} \approx 9.9$. So the answer is C.

Question:
What is the perimeter of quadrilateral CBDE? Choices: A. 33.0; B. 34.0; C. 35.0; D. 32.0

Rational:
The perimeter of quadrilateral CBDE includes sides CB, BD, DE, and EC. Given CB = 7.0, BD = 10.0, and knowing quadrilateral CBDE has parallel and equal opposite sides, DE = CB and EC = BD. Thus, DE = 7.0 and EC = 10.0. The perimeter = CB + BD + DE + EC = 7.0 + 10.0 + 7.0 + 10.0 = 34.0 units. So the answer is B.

Figure 27: The function prompt for GPT-4V and the generated questions and rationals.

Diagram:

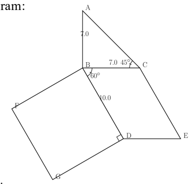

Caption:

Firstly, trace a Right Triangle ABC. Secondly, attached to edge CB, draw a Quadrilateral with opposite sides parallel and equal in length CBDE. Thirdly, joined to edge DB, render a Square DBFG. The measurement of angle ACB is 45º. The angle DBC measures 60º. Angle BDG measures 90º in size. The distance between points A and B is 7.0. The segment CB spans 7.0 units. Side DB spans 10.0 units.

Prompt for Plane Geometry Problems:

Here is some more supplementary information of the diagram I give you: "{caption}"
Please first watch the diagram and ask a question that can be correctly answered only by seeing the diagram.
Then you should correctly analysis the question and give the answer.
The reasoning process should not use "According to the caption" or something like that.
Next, you should give 3 other hard false choices along with the correct one.

You should totally provide 3 questions.
The type of questions is multi-choice.

You should strictly follow this format and order (end every problem with ####):
QUESTION: What is the height of the trapezium ABCD?
ANALYSIS: Since we know the length of AB and the angle CBA, we can derive the height of the trapezium ABCD. The height should be AB \times sin(\angle CBA) = 11.7 * sin(60) = 10.1, so the answer is 11.7
ANSWER: B. 11.7
CHOICE: A. 11; B. 11.7; C. 12; D. 8 ####

Question & Rationale Generated by GPT-4V:

Question:
What is the length of square side FG? Choices: A. 10.0; B. 10.1; C. 9.9; D. 10.5

Rational:
Since FG is a side of square DBFG, and the properties of a square dictate that all sides are equal in length, the length of FG must be the same as DB which is given as 10.0 units. So the answer is A.

Question:
What is the length of diagonal AC in triangle ABC? Choices: A. 10.1; B. 9.8; C. 9.9; D. 10.0

Rational:
In right triangle ABC with sides AB = 7.0 and BC = 7.0 units, and angle ACB = 45°, the triangle is isosceles. The length of diagonal AC can be calculated using the Pythagorean theorem: $AC = \sqrt{}(AB^2 + BC^2) = \sqrt{}(7.0^2 + 7.0^2) = \sqrt{98} \approx 9.9$. So the answer is C.

Question:
What is the perimeter of quadrilateral CBDE? Choices: A. 33.0; B. 34.0; C. 35.0; D. 32.0

Rational:
The perimeter of quadrilateral CBDE includes sides CB, BD, DE, and EC. Given CB = 7.0, BD = 10.0, and knowing quadrilateral CBDE has parallel and equal opposite sides, DE = CB and EC = BD. Thus, DE = 7.0 and EC = 10.0. The perimeter = CB + BD + DE + EC = 7.0 + 10.0 + 7.0 + 10.0 = 34.0 units. So the answer is B.

Figure 28: The geometry prompt for GPT-4V and the generated questions and rationals.

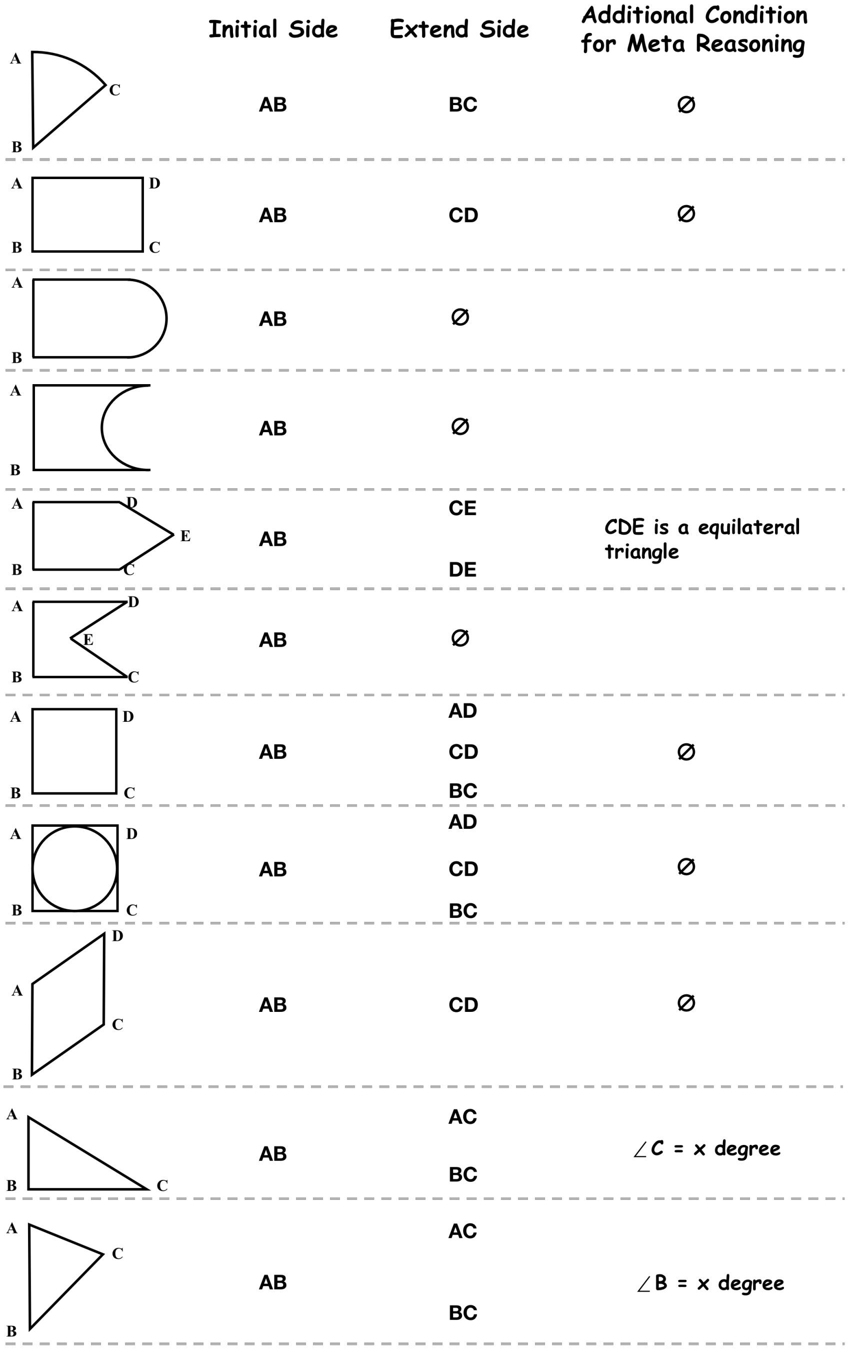

Initial Side	Extend Side	Additional Condition for Meta Reasoning
AB	BC	∅
AB	CD	∅
AB	∅	
AB	∅	
AB	CE DE	CDE is a equilateral triangle
AB	∅	
AB	AD CD BC	∅
AB	AD CD BC	∅
AB	CD	∅
AB	AC BC	∠C = x degree
AB	AC BC	∠B = x degree

Figure 29: The initial side, extend side, and additional conditions for meta-reasoning of each basic shape. Some special shapes are not extended and only appear in the last position of the generation sequence, thus their extend side is ∅.